Astrophysical Journal
Preprint typeset using LaTeX style emulateapj v. 01/23/15



# EVOLUTION OF FINITE VISCOUS DISKS WITH TIME-INDEPENDENT VISCOSITY

G. V. Lipunova
Lomonosov Moscow State University, Sternberg Astronomical Inst., Universitetski pr. 13, Moscow 119991, Russia; galja@sai.msu.ru
(Received February 8, 2015; Accepted March 30, 2015; Published May 5, 2015)

## ABSTRACT

We find the Green's functions for the accretion disk with the fixed outer radius and time-independent viscosity. With the Green's functions, a viscous evolution of the disk with any initial conditions can be described. Two types of the inner boundary conditions are considered: the zero stress tensor and the zero accretion rate. The variable mass inflow at the outer radius can also be included. The well-known exponential decline of the accretion rate is a part of the solution with the inner zero stress tensor. The solution with the zero central accretion rate is applicable to the disks around stars with the magnetosphere's boundary exceeding the corotation radius. Using the solution, the viscous evolution of disks in some binary systems can be studied. We apply the solution with zero inner stress tensor to outbursts of short-period X-ray transients during the time around the peak. It is found that for the Kramers' regime of opacity and the initial surface density proportional to the radius, the rise time to the peak is $t_{\rm rise} \approx 0.15\, r_{\rm out}^2/\nu_{\rm out}$ and the $e$-folding time of the decay is $t_{\rm exp} \approx 0.45\, r_{\rm out}^2/\nu_{\rm out}$. Comparison to non-stationary $\alpha$-disks shows that both models with the same value of viscosity at the outer radius produce similar behaviour on the viscous time-scale. For six bursts in X-ray novae, which exhibit fast-rise-exponential-decay and are fitted by the model, we find a way to restrict the turbulent parameter $\alpha$.
*Subject headings:* accretion, accretion disks – binaries: general – methods: analytical

## 1. INTRODUCTION

The accretion processes are recognized to power many astrophysical sources, which are observable due to the release of energy when matter is spiralling down into the gravity well. The study of viscous accretion disks as underlying mechaisms for the extraction of potential gravitational energy began with the works of Lynden-Bell (1969); Shakura & Sunyaev (1973), Novikov & Thorne (1973, pp.343-450).

Time-dependent problems for the accretion disks arise when describing a wide variety of outburst phenomena, observed in the accreting sources, i.e. binary systems with mass transfer and galactic nuclei, and systems with planet formation. It is usually possible to consider separately the vertical and radial structure of an accretion disk due to significantly different characteristic time-scales. In such a case the time-dependent radial structure of a disk can be described by a second-order partial differential equation, which is a consequence of the angular momentum and mass conservation. The energy conservation in a geometrically thin optically thick disk is provided by the local balance of the viscous heating and radiative cooling.

The basic equation of the viscous evolution, Eq. (1) or (6) below, describes the viscous angular momentum flux along the disk radius. This is a diffusion type equation with a variable 'diffusion' coefficient. Choice of an analytic approach to solve the equation depends on the nature of the viscosity involved. The preferential way of describing viscosity in astrophysical disks, although not exclusive, is to use $\alpha$-viscosity (Shakura 1973; Shakura & Sunyaev 1973), i.e., the proportionality of the viscous stress tensor to the total pressure in the disk. One can generally assume that the kinematic viscosity $\nu$ is a product of two power functions: one function of radius and another of some local physical parameter, the latter usually represented by the surface density.

The boundary conditions imposed on the accretion disk are important. While the outer boundary can be a freely expanding surface due to the spreading of the matter corresponding to the outward viscous angular momentum flux, in some situations certain conditions should be posed at some distance from the accreting object. Disks in the binary systems are the main focus for such models.

In a binary system, the tidal torques, acting inside the Roche lobe of the accreting object, truncate the disk and provide a sink for the angular momentum. Papaloizou & Pringle (1977) show that the effective tidal radius is close to the Roche lobe: $\sim 0.9$ of the mean radius of the Roche lobe, well coinciding with the largest non-intersecting periodic orbits in the restricted three-body problem (Paczynski 1977). Numerical models confirm that most of the tidal torque is applied in a narrow region at the edge of the disk, where perturbations become nonlinear and strong spiral shocks appear (see Pringle 1991; Ichikawa & Osaki 1994; Hameury & Lasota 2005, and references therein). In the present study, we leave aside the outer disk radius variations and other manifestations of the tidal interactions in the binary except for the disk truncation. We confine ourselves to searching for a solution to a problem of the viscous evolution of an accretion disk with the constant outer radius.

We investigate a geometrically thin, axisymmetric Keplerian finite accretion disk with a viscosity in the form $\nu \propto r^b$, which is time-independent. We obtain Green's functions (19), (22), (31), and (32), which are the kernels in the integrals (20), (21), and (35) to compute the viscous angular momentum flux[1] $F$ and the accretion rate $\dot{M}$. The method of Green's functions allow one to compute $\Sigma(r,t)$ and $\dot{M}(r,t)$ for arbitrary initial surface density distributions. Different boundary conditions are considered: no stress or no accretion at the inner boundary, which is located at the zero radial coorinate, zero or time-dependent mass inflow at the outer boundary.

It is beleived that the mechanism of bursts in X-ray novae involves the thermal instability connected with opacity variations in the disks, as in dwarf novae. When a burst is ignited, and a sufficient portion of the disk is in the hot state, the vis-

[1] The couple $g$ of Lynden-Bell & Pringle (1974).

cous diffusion starts to govern the evolution, driving the characteristic rise and drop of the accretion rate onto the central object. It is a question, which probably allow no universal answer, why X-ray novae light curves have different profiles and pecularities. If the disk is not very large, as it happens in short-period X-ray transients, its whole body is likely to be engaged in the viscous evolution. It has been shown that an episodic mass input at the outer radius causes the fast-rise-exponential-decay (FRED) profile due to the viscous evolution (Wood et al. 2001). Using the Green's function, one can explore the situation with an arbitrary initial distribution of the matter. Actually, as we show in the present study after obtaining the Green function, for realistic initial density distributions and for the case with the zero inner viscous stress, the evolution is generally a FRED. It is interesting to compare the results of the model with what happens in the $\alpha$-disks, the prevalent model for the disks' turbulence in the stellar binaries.

The second case, when the viscous stress is non-zero at the center, applies to the disks with the central source of the angular momentum, e.g., rotating stars with magnetosphers. If the magnetosphere's radius is large enough, the matter has a super-Keplerian angular momentum at its boundary. Different regimes for such disks have been proposed: propellers and 'dead' disks. Using the Green founction, the disks of constant mass that evolve to dead disks can be described.

In binary systems the mass transfer rate is a key factor. At some stages it can be considered negligible comparing to the accretion rate in the disk. In other systems, mass transfer variations may cause the activity in the disk. The case of time-dependent mass transfer, which includes the constant transfer rate as a particular case, can be also studied analytically if $\nu \propto r^b$. Using the Green's functions, it is possible to express $\Sigma(r,t)$ and $\dot{M}(r,t)$ for any outer boundary conditions (for any $\dot{M}_{\rm out}(t)$) as well as for any initial conditions.

In Section 2, we present the viscous evolution equation and review its known solutions for accretion disks. In Section 3, the Green's functions are found for different inner and outer boundary conditions. An analytic way to calculate the disk evolution with the variable mass transfer at the outer radius is presented; the features of a radiating dead disk are considered. In Section 4, a stage of decaying accretion is dealt with and a comparison to the $\alpha$-viscosity models is made. Application to the FRED light curves of short-period X-ray transients is presented in Section 5. The last sections are dedicated to the discussion and summary.

## 2. VISCOUS ACCRETION DISK EQUATION

The equation of the viscous evolution in the accretion disk is the diffusion-type equation (e.g., Kato et al. 1998):

$$\frac{\partial \Sigma}{\partial t} = \frac{1}{r}\frac{\partial}{\partial r}\left[\frac{1}{\partial(\omega r^2)/\partial r}\frac{\partial}{\partial r}(W_{r\varphi} r^2)\right], \qquad (1)$$

where, among the standard designations of the time, radius, angular speed, and the surface density we have the component of the viscous stress tensor $w_{r\varphi}$, integrated over the full thickness of the disk

$$W_{r\varphi}(r,t) = 2\int_0^{z_0} w_{r\varphi}\,{\rm d}z\,,$$

where $z_0$ is the half-thickness of the disk at radius $r$, and the stress tensor is related to the differential rotation of gas masses by the kinematic viscosity $\nu$ as follows:

$$w_{r\varphi} = -\rho\,\nu\,r\,\frac{{\rm d}\omega}{{\rm d}r}\,. \qquad (2)$$

For the Keplerian disks ${\rm d}\omega/{\rm d}r = -(3/2)\omega_{\rm K}/r$, and we rewrite

$$W_{r\varphi}(r,t) = 3\,\omega_{\rm K}\int_0^{z_0}\nu\,\rho\,{\rm d}z\,. \qquad (3)$$

With the formula for the surface density

$$\Sigma(r,t) = 2\int_0^{z_0}\rho(r,z,t)\,{\rm d}z\,, \qquad (4)$$

assuming that $\nu$ is independent on $z$, we have

$$W_{r\varphi}(r,t) = \frac{3}{2}\,\omega_{\rm K}\,\nu\,\Sigma\,. \qquad (5)$$

It is convenient to introduce a new independent variable $h(r) = v_\varphi(r)\,r = \omega\,r^2$ – the specific angular momentum. Then, for the Keplerian disk, equation (1) can be rewritten as:

$$\frac{\partial\Sigma}{\partial t} = \frac{3}{4}\frac{(G\,M)^2}{h^3}\frac{\partial^2(\Sigma\,\nu\,h)}{\partial h^2}\,, \qquad h \equiv h_{\rm K}\,. \qquad (6)$$

The acknowledged approach is to solve the disk evolution equation for the variable proportional to the full viscous torque acting between the adjacent rings in the disk, $\omega_{r\varphi}\cdot z\,2\pi r\cdot r$. This way, the boundary conditions are easy to express. From the above expressions, the following relation between $F = 2\,\pi\,W_{r\varphi}r^2$ and the accretion rate can be obtained:

$$-\,2\,\pi\,\Sigma\,v_r\,r \;\equiv \dot{M}(r,t) = \frac{\partial F}{\partial h}\,, \qquad (7)$$

where the radial velocity $v_r$ is negative.

One chooses a procedure to solve (6) provided the form of $\nu = \nu(r,\Sigma)$ is known. This form is determined by the physical conditions in the disk. For example, the vertical structure can be solved for the $\alpha$-disk, and the required relation between $\nu$ and $\Sigma$ can be found. Let us give a perspective of some studies (mainly analytic) of the viscously evolving accretion disks. They differ in respect of the viscosity prescription and boundary conditions. The analytic solutions are the benchmarks for more sophisticated and involved numerical models.

### 2.1. *Viscosity* $\nu \propto r^b$

For the kinematic viscosity in the form $\nu \propto r^b$, the equation of the viscous evolution (6) becomes a linear partial differential equation. In 1952 Lüst obtained particular solutions to the equation proposed by his teacher von Weizsäcker (1948) and described the principles to determine the general solution for the infinite and finite problems.

For the accretion disks that can extend *infinitely*, Lynden-Bell & Pringle (1974) (hereafter LP74) find, for the two types of the inner boundary conditions, the Green's functions that provide means to describe the whole development of the disk. The inner radius of the disk is zero in their exact solution. The long-term self-similar evolution of the accretion rate goes as a power-law $\dot{M} \propto t^{-(l+1)}$ with a parameter $l < 1$ (see also Appendix A).

Pringle (1991) considers the properties of an infinite accretion disk with a central source of the angular momentum using

the Green-function technique. A related problem is solved by Tanaka (2011) who finds the Green's function for an infinite disk with the boundary conditions posed at the finite inner radius.

King & Ritter (1998) consider a *finite* disk with the viscosity constant over the radius and in time and derive the exponential decay of the accretion rate in the disk.

Zdziarski et al. (2009) study the mass flow rate through a disk resulting from a varying mass-supply rate, derive the Green's function for the accretion-rate and its Fourier transform. By means of numerical simulations, they investigate a *finite* disk, residing between non-zero $r_{\rm in}$ and $r_{\rm out}$, with the non-zero accretion rate at the outer radius. Tanaka et al. (2012) find general Green's function for an explicit dependence of the inner boundary $r_{\rm in}$ on time and a non-zero mass across $r_{\rm in}$.

In the present work, we study analytically a finite accretion disk with the zero $r_{\rm in}$ and find an analytic solution describing its whole evolution, from the rise to decay. For the case of the zero stress tensor in the disk center and the mass deposition at the outer disk edge, the Green's function of the problem is found in Wood et al. (2001).

### 2.2. *Viscosity* $\nu \propto \Sigma^a r^b$

Similarity solutions of the first kind of the non-linear differential equation (Barenblatt 1996) have been found at the "decaying-accretion stage," when the total angular momentum of an *infinite* disk is constant (Pringle 1974, 1981). Accretion rate is found to decrease as $\propto t^{-5/4}$ for the Thomson opacity, and as $\propto t^{-19/16}$ for the Kramers' opacity (see also Filipov 1984; Cannizzo et al. 1990). Lyubarskij & Shakura (1987) obtain self-similar solutions that describe separately three stages of the disk evolution. The first two are the self-similar solutions of the second kind: the initial movement of the inner edge of a ring of matter toward the center and the rise of the accretion rate in the center ($\dot{M} \propto t^{2.47}$ for the Kramers' opacity and $\propto t^{1.67}$ for the Thomson opacity). The third stage is the decay of the accretion and corresponds to the solution of Pringle (1974). The first two stages of Lyubarskij & Shakura (1987) may be applicable to the *finite* disks when the conditions at the distant outer boundary do not affect the behaviour of the disk near the center.

Lin & Pringle (1987) derive an analytic self-similar solution for a disk subject to the gravitational instability, which transfers mass and angular momentum in the disk, for which $\dot{M} \propto t^{-6/5}$, and a numerical solution for the whole evolution. Lin & Bodenheimer (1982) found a self-similar solution for $\nu \propto \Sigma^2$, if the viscosity is due to the action of convectively driven turbulent viscous stresses ($\dot{M} \propto t^{-15/14}$).

Accretion disks with a central source of angular momentum and no mass transfer through the inner boundary were considered by Pringle (1991) who derived a self-similar solution (see also Ivanov et al. (1999)). Rafikov (2013) in the extensive study of the circumbinary disks around supermassive black holes obtained self-similar solutions for the disks with a possible mass transfer across the orbit of the secondary black hole.

For a *finite* disk, the radial and temporal solution is obtained by Lipunova & Shakura (2000) yielding $\dot{M} \propto t^{-10/3}$ for the Kramers' opacity and $\dot{M} \propto t^{-5/2}$ for the Thomson opacity.

In the context of the self-similarity solutions, we would like to note that for an advection-dominated infinitely expanding accretion flow, Ogilvie (1999) obtains by similarity methods a time-dependent solution with the conserved total angular momentum.

## 3. EVOLUTION OF THE FINITE DISK WITH STEADY VISCOSITY

If the kinematic viscosity $\nu$ is not a function of $\Sigma$ and is a function of the radius alone, we arrive at the linear differential equation (6). We write the kinematic viscosity as

$$\nu = \nu_0\, r^b\,. \tag{8}$$

Then Eq. (6) for the dependent variable $F$ is as follows

$$\frac{\partial F}{\partial t} = \frac{3}{4}\,\nu_0\, h^{2b-2}\,(G\,M)^{2-b}\,\frac{\partial^2 F}{\partial h^2}\,, \tag{9}$$

where

$$F = 2\,\pi\, W_{r\varphi}\, r^2 = 3\,\pi\, h\,\Sigma\,\nu_0\, r^b\,. \tag{10}$$

We rewrite (9) in the form similar to that in LP74:

$$\frac{\partial^2 F}{\partial h^2} = \frac{1}{4}\left(\frac{\kappa}{l}\right)^2\, h^{1/l-2}\,\frac{\partial F}{\partial t}\,, \tag{11}$$

where the constants are defined as follows:

$$\frac{1}{2\,l} = 2 - b\,, \qquad \kappa^2 = \frac{16\,l^2}{3\nu_0\,(G\,M)^{1/2l}}\,. \tag{12}$$

There is a degeneracy of the index $l$ at $b = 2$. But it is only apparent as $l$ enters equation (11) in the denominators. Value $b = 2$ corresponds to the change of the class of functions, which satisfy the differential equation, and is left out of the following consideration. In the case of $b = 2$ the viscous time is constant over the disk radii $t_{\rm vis} \propto r^2/\nu_o r^b$. We limit ourselves to the finite positive values of $l$ and the Keplerian disks.

In the astrophysical hot accretion disks, the turbulent viscosity is at work. According to the Prandtl concept (Prandtl 1925), the kinematic turbulent viscosity is an averaged product of the two random values: $\nu_{\rm t} = \overline{l_{\rm t}\,\upsilon_{\rm t}}$, where $l_{\rm t}$ and $\upsilon_{\rm t}$ are the path and speed of the turbulent motion. For the component of the viscous stress tensor we write $w_{r\varphi} = -\rho\,\nu_{\rm t}\,r\,{\rm d}\omega/{\rm d}r$. Following the Prandtl consideration, $\upsilon_{\rm t} = -l_{\rm t}\,r\,{\rm d}\omega/{\rm d}r$, which leads to $w_{r\varphi} = \rho\,\overline{\upsilon_{\rm t}^2}$. Shakura (1973) proposed the $\alpha$-disks: $w_{r\varphi} = \alpha\,\rho\,\upsilon_{\rm s}^2$. From the hydrostatic balance one derives the sound speed $\upsilon_{\rm s} \approx \omega\,r\,(z_0/r)$ and obtains for a Keplerian disk $\nu_{\rm t} \approx 2/3\,\alpha\,h\,(z_0/r)^2$. If the relative half-thickness of the $\alpha$-disk is invariable then $b = 1/2$ and $l = 1/3$. This value of $b$ takes place for the '$\beta$-viscosity disks' with $\nu = \beta\,h$, suggested by Duschl et al. (2000) to act in the protoplanetary and galactic disks. The standard model of the $\alpha$-disk implies that $h/r$ varies with $r$ and $\Sigma$.

Let us find the Green's function of the linear equation (11) with the specific boundary conditions at the boundaries. A Green's function or a diffusion kernel is a reaction of the system to the delta impulse, in other words, the Green's function is the solution to the differential equation with the initial condition $F(x,0) = \delta(x - x_1)$, where $\delta(x - x_1)$ is the Dirac delta function. We search a solution by separating the variables, $F(h,t) = f(h_{\rm out}\,\xi)\,\exp(-s\,t)$, where $s$ is a constant and $h_{\rm out}$ is the outer disk radius. Substituting this into (11), we get

$$\frac{{\rm d}^2 f(\xi)}{{\rm d}\xi^2} + \frac{1}{4}\left(\frac{k}{l}\right)^2\,\xi^{1/l-2}\,f(\xi) = 0\,, \tag{13}$$

where $k^2 = \kappa^2 h_{\rm out}^{1/l} s$. This is a Lommel's transformation of the Bessel equation, which can be derived by introducing a new independent variable $x = \xi^{1/2l}$. A particular solution is represented as

$$F_k(x,t) = e^{-st}\,(kx)^l\,[A\,J_l(kx) + B\,J_{-l}(kx)]$$

(Lüst 1952), where $J_l$ and $J_{-l}$ are the Bessel functions of a non-integer order. If $l$ is an integer number, the Bessel functions of the second kind should be used instead of $J_{-l}$. For $b = 2$, the solution is no more a Bessel function (see Appendix I of Kato et al. 1998). The value $b = 2$ marks a situation when the characteristic viscosity time $r^2/\nu$ is constant over the radius. We do not consider this case in the present study.

A general solution for an infinite problem is a superposition of particular solutions and is expressed by LP74 as an integral over all positive values of $k$: $F(x,t) = \int_0^\infty F_k(x,t)\,{\rm d}k$. For a problem inside a finite interval, a general solution is a superposition of particular solutions and is expressed as an infinite sum (Lüst 1952):

$$F(x,t) = \sum_{i=1}^{\infty} e^{-t\,k_i^2\,\kappa^{-2}\,h_{\rm out}^{-1/l}}\,(k_i\,x)^l\,[A_i\,J_l(k_i\,x) + B_i\,J_{-l}(k_i\,x)]\,, \tag{14}$$

where constants $k_i$, $A_i$. and $B_i$ are to be defined from two boundary conditions and one initial condition. The dimensionless coordinate $x$ lies in the interval $[0,1]$, while the physical coordinate $h$ (specific angular momentum) lies inside $[0, h_{\rm out}]$. The outer boundary condition, which sets the accretion rate at the outer radius of the disk, can be written as follows

$$\frac{\partial F}{\partial h} = \dot{M}_{\rm out}(t) \;\text{ at }\; h = h_{\rm out}\,. \tag{15}$$

In the simplest case, the homogeneous outer-boundary condition corresponds to the zero mass-inflow rate at the outer boundary. As this happens, the viscous angular momentum flux $F$ takes some non-zero value, which implies withdrawal of the angular momentum at the outer boundary. This corresponds to the situation of the disk in the binary system, when the angular momentum is removed from the outer edge of the disk by the tidal action of the secondary.

At $x = 0$, one trivial inner boundary condition $F(x,t) = 0$ approximates the structure for the so-called 'standard' disk, for which the absence of the viscous stresses at the disk inner edge is assumed. Another simple case, $\partial F/\partial h = 0$ at $x = 0$, describes the situation of no accretion through the inner disk edge. This case is applicable for the stars with strong magnetosphere, when the Alfvén radius is greater than the corotation radius, impeding the accretion of the matter. We consider these two cases separately.

### 3.1. *The case of zero viscous stress at the inner boundary and zero accretion rate at $r_{\rm out}$*

First, we consider the case of the zero viscous stress at the inner boundary. Approximately, this corresponds to the solution $F(x,t) = 0$ at $x = 0$ and only the coefficients at $J_l$-terms in (14) remain non-zero. Thus, sum (14) at $t = 0$ becomes

$$F(x,0) = \sum_{i=1}^{\infty} (k_i\,x)^l\,A_i\,J_l(k_i\,x)\,. \tag{16}$$

We assume the zero accretion rate at $r_{\rm out}$. Such boundary condition approximates the situation of the low mass-transfer from the secondary in the binary system, for example, when the accretion rate in the disk is much higher than the mass transfer rate during an outburst. Dropping the time part of the solution, we arrive at condition (15) required for every term in the sum (16), which can be rewritten as follows:

$$l\,J_l(k_i) + k_i\,J_l'(k_i) = 0\,. \tag{17}$$

Thus, the general solution for the case of zero viscous stress tensor at the center and zero accretion rate at the outer boundary is the sum (14), where $B_i = 0$ and $k_i$ are the positive roots of the transcendental equation (17). To define $A_i$ from the initial condition, the finite Hankel transforms are used.

The series $\sum_{i=1}^{\infty} k_i^l\,A_i\,J_l(k_i\,x)$ with condition (17) are known as the Dini's series (see Watson 1944, §18.11). Function $f(x) = F(x,0)\,x^{-l}$ can be expressed as the Dini's expansion if the function satisfies the Dirichlet conditions in the interval and the coefficients are defined as $k_i^l A_i = 2\,\bar{f}_J(k_i)\,J_l^{-2}(k_i)$ (Watson 1944; Sneddon 1951) with the finite Hankel transform

$$\bar{f}_J(k_i) = \int_0^1 x\,f(x)\,J_l(k_i\,x)\,{\rm d}x\,,$$

where $f(x) = F(x,0)\,x^{-l}$. We look for a solution for the $\delta$-function as the initial condition: $F(x,0) = \delta(x - x_1)$. Using the properties of the Dirac function, we obtain

$$k_i^l\,A_i = 2\,x_1^{1-l}\,\frac{J_l(k_i\,x_1)}{J_l^2(k_i)}\,. \tag{18}$$

Thus, for the specific boundary conditions, we derive the Green's function, which is the solution to (11) with $\delta$-function as the initial distribution

$$G(x,x_1,t) = 2\,x^l\,x_1^{1-l}\,\sum_i e^{-t\,k_i^2\,\kappa^{-2}\,h_{\rm out}^{-1/l}}\,\frac{J_l(k_i\,x_1)\,J_l(k_i\,x)}{J_l^2(k_i)}\,, \tag{19}$$

where $k_i$ are the positive roots of Eq. (17) and $x = (h/h_{\rm out})^{1/2l}$. The function is plotted in Fig. 1 for consecutive times. The curve for time $t_3$ corresponds to the maximum accretion rate in the center. It is plotted at $t_3 = t_{\rm max}^{\infty}$ given by (25) below.

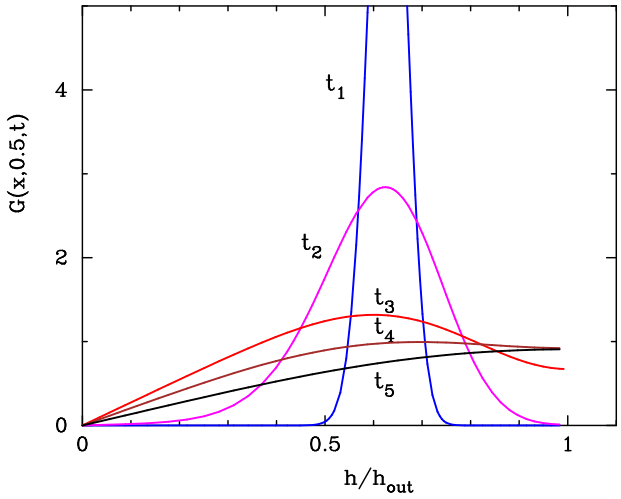


FIG. 1.— Green's function for the finite accretion disk with the zero viscous stress in the center at five moments of time $t_1 = 0.001$, $t_2 = 0.01$, $t_3 = t_{max}^{\infty} = 3/64$, $t_4 = 0.1$, $t_5 = 0.3$. Initial spike was at position $x_s = (h/h_{\rm out})^{1/2l} = 0.5$. Constants $\kappa = 1$, $l = 1/3$.

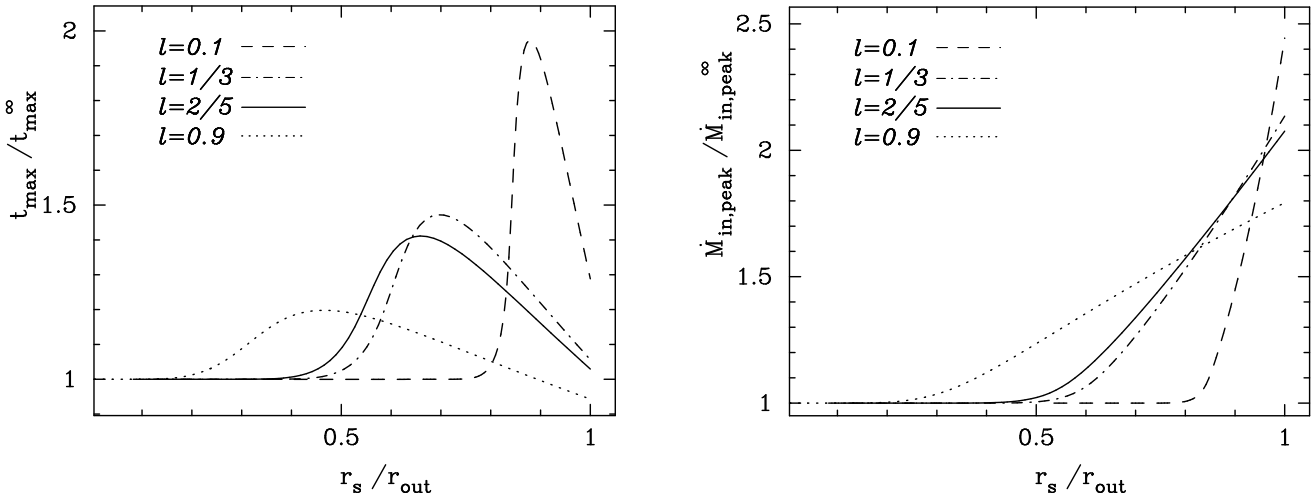


FIG. 2.— Left: ratio of the time when the accretion rate peaks in the finite disk to that in the infinite disk versus the position of the initial thin ring. Right: ratio of the peak accretion rate in the finite disk to that in the infinite disk as a dependence on the initial ring position.

Given the dimensional initial distribution $F(x,0)$ in the finite accretion disk, the distribution of $F$ at any $t > 0$ is

$$F(x,t) = \int_0^1 F(x_1,0)\, G(x,x_1,t)\, \mathrm{d}x_1 \,. \qquad (20)$$

The accretion rate can be found from

$$\dot{M}(x,t) = \int_0^1 F(x_1,0)\, G_{\dot{M}}(x,x_1,t)\, \mathrm{d}x_1 \Big/ h_{\rm out} \,, \qquad (21)$$

where the Green's function for the accretion rate

$$G_{\dot{M}}(x,x_1,t) \equiv \frac{\partial G(x,x_1,t)}{\partial x^{2l}} = \\ = \frac{(x\,x_1)^{1-l}}{l} \sum_i e^{-t\,k_i^2\,\kappa^{-2}\,h_{\rm out}^{-1/l}}\, k_i\, \frac{J_l(k_i\,x_1)\,J_{l-1}(k_i\,x)}{J_l^2(k_i)} \,. \qquad (22)$$

Functions $G$ and $G_{\dot{M}}$ are found by Wood et al. (2001) for the case $x_1 = 1$ along with an analytical form obtained from the asymptotic forms for small and large $t$.

One can express the initial $F$, proportional to the disk mass, from the initial distribution of the surface density, using (5) and (12):

$$F(x,0) = \frac{16\,\pi\,l^2}{\kappa^2\,h^{1/l}}\, r^2\, \Sigma(r)\, h \qquad (23)$$

where $r = h^2/GM$ and $h = h_{\rm out}\, x^{2l}$.

### 3.1.1. *Spike-like and power-law initial distribution of the viscous stresses*

Let the initial mass be located at some radius $r_s$ where the Keplerian specific angular momentum is $h_s = x_s^{2l}\, h_{\rm out}$, and the mass of the infinitely thin ring is $M_{\rm disk}$, $h_{\rm out}$ is the maximum possible specific angular momentum of the matter.

The surface density of the $\delta$-ring is

$$\Sigma(r) = \frac{M_{\rm disk}}{2\,\pi\,r_s}\,\delta(r-r_s) = \frac{M_{\rm disk}}{8\,\pi\,l\,r_s^2}\,x_s\,\delta(x-x_s) \,.$$

We take into account that $\delta(r-r_s) = \delta(x-x_s)\mathrm{d}x/\mathrm{d}r$ and $r = x^{4l}\, r_{\rm out}$. Applying (23), we obtain

$$F(x,0) = \frac{2\,l}{\kappa^2}\, M_{\rm disk}\, h_{\rm out}^{1-1/l}\, x_s^{2l-1}\, \delta(x-x_s) \qquad (24)$$

and the accretion rate evolution is as follows

$$\dot{M}(x,t) = \frac{M_{\rm disk}}{t_{\rm vis}}\, x_s^{2l-1}\, G_{\dot{M}}(x,x_s,t) \,,$$

where we designate

$$t_{\rm vis} = \frac{\kappa^2\, h_{\rm out}^{1/l}}{2\,l} = \frac{8\,l}{3}\,\frac{r_{\rm out}^2}{\nu(r_{\rm out})} \,.$$

The time $t_{\rm max}$ of the maximum and its accretion rate in the disk center $\dot{M}_{\rm in,peak}$ are of order of those for the infinite disks. Using the solution of LP74, we find the time of the accretion rate peak for the infinite disk

$$t_{\rm max}^{\infty} = \frac{\kappa^2\, h_s^{1/l}}{4\,(1+l)} = \frac{4\,l^2}{3\,(1+l)}\,\frac{r_s^2}{\nu(r_s)} \qquad (25)$$

and value $\dot{M}_{\rm in,peak}^{\infty}$ (A1). The numerical factor in (25) is presented in Table 1 for various, physically motivated values of $l$. In Fig. 2 the ratios of maximum times and accretion rates for the finite and infinite disk are shown for several cases of $l$. The ratios approach 1 for $x_s \ll 1$ – the disk 'does not feel' the boundary at the time when the accretion rate peaks.

If the initial surface density is distributed as a power-law with radius $\Sigma \propto r^{\alpha_\Sigma}$, we use the following expression in Eq. (23):

$$\Sigma(r) = \frac{M_{\rm disk}}{2\,\pi\,r^2}\,\frac{(\alpha_\Sigma+2)\,(r/r_2)^{\alpha_\Sigma+2}}{1-(r_1/r_2)^{\alpha_\Sigma+2}} \,,$$

assuming the mass of the disk is enclosed between the radii $r_1$ and $r_2$.

In Fig. 3 the variation of the accretion rate at the disk center is presented for three different initial distributions of $F$ (see Fig. 4): two narrow top-hats ($\alpha_\Sigma = 1/2l - 5/2$) with different $r_1$ and $r_2$ and the one corresponding to $\Sigma(r,0) \propto r$. All three initial distributions are constructed for the same initial mass of the disk $M_{\rm disk} = 1$. The evolution of a thin ring located far from the outer disk edge has a characteristic power-law interval, when the disk behaves as if it was infinite. The interval

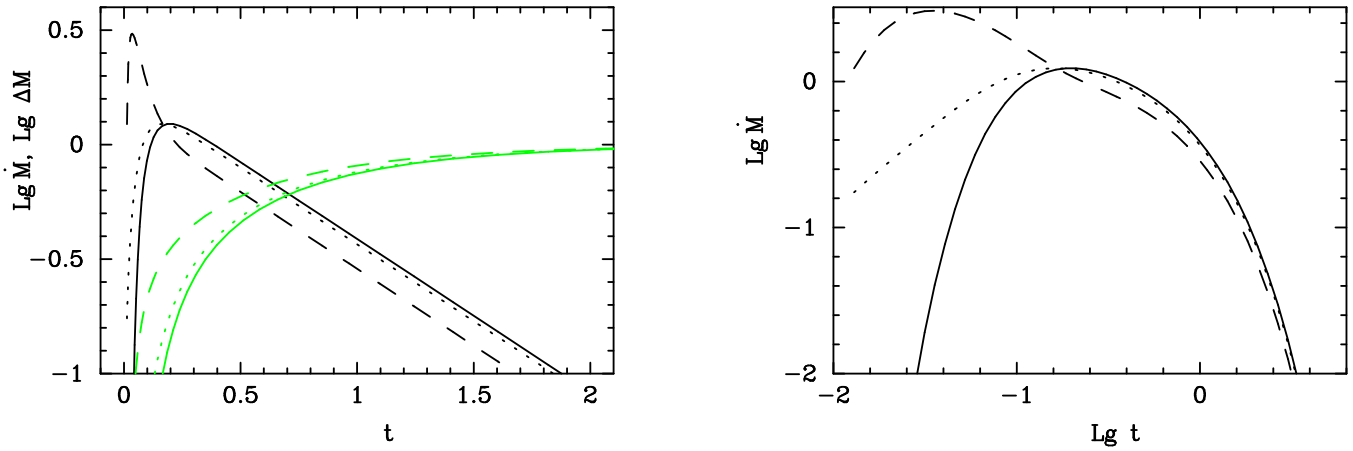


FIG. 3.— The inner accretion rate variation (the black curves with a peak) for three initial distributions of $F(h)$ shown in Fig. 4. The initial mass of the disk is the same in all cases. On the left panel, the cumulative accreted mass is shown by the monotonic (green in the electronic version) curves. The dashed curve has a power-law interval, which is clearly seen on the right panel. Constants $M_{\rm disk} = 1$, $h_{\rm out} = 1$, $\kappa = 1$, $l = 1/3$, $t_{\rm vis} = 3/2$.

lasts about $t_{\rm max}[1 - (h_{\rm s}/h_{\rm out})^{1/l}]$. If $\Sigma(r, 0) \propto r$, the mass of the disk at $t = 0$ is enclosed mainly in the outer parts, because it grows as the cube of the radius. As expected, the accretion rate's evolution after the peak depends weakly on the peculiarities of the initial distribution of mass in the disk (compare the dotted and solid line in Fig. 3), as long as its bulk was similarly positioned.

### 3.1.2. *Disk luminosity*

The viscous heating in the disk (its half) is found from $F$:

$$Q_{\rm vis} = \frac{3}{8\,\pi}\,\frac{F\,\omega_{\rm K}}{r^2}\,, \qquad (26)$$

which can be equated to $\sigma T_{\rm eff}^4$ assuming the local energy balance.

In the center of the disk, the quasi-stationary distribution develops soon and the accretion rate is constant over radii: $F(t) = \dot{M}(t)\,h$. The zone of constant $\dot{M}$ expands over time.

The viscous heating (26) with the quasi-stationary distribution of $F$ diverges at the zero coordinate. In the real astrophysical disks, the inner radius of the disk is a finite value $r_{\rm in} \neq 0$. Note that integrating (26) over the disk surface from $r_{\rm in}$ to $r_{\rm out}$ also yields the incorrect result for the total power released in the disk. (As a remark, the integration of (26) gives the correct result for the case of the zero accretion rate at the center, see § 3.2.1).

In fact, setting $F(r_{\rm in}) = 0$ at the finite radius $r_{\rm in}$ leads to a time-independent correction of $F$ near $r_{\rm in}$. This correction is found for the infinite disks by Tanaka (2011) and represents the classical factor $(1 - \sqrt{r_{\rm in}/r})$. Naturally, the correction holds for a finite disk. It follows that the bolometric luminosity can be calculated via the classical formula $L_{\rm bol} = G\,M\,\dot{M}/(2r_{\rm in})$ at times $t > t_{\rm vis}(r_{\rm in}/r_{\rm out})^{2-b}$ with the first term in the correction of order of $(r_{\rm in}/r_{\rm out})\,(t_{\rm vis}/t)^{1/(2-b)}$ for earlier times. For the disks in the stellar binary systems, usually, ratio $r_{\rm in}/r_{\rm out} << 1$, and we are safe to calculate $L_{\rm bol}$ by the classical formula with $\dot{M} = \dot{M}(0, t)$ found from (21).

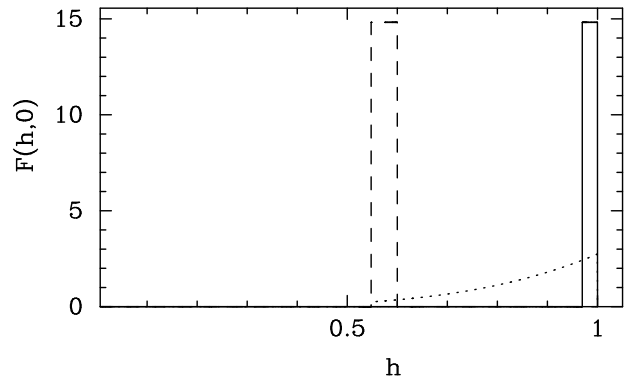


FIG. 4.— Three initial distributions of $F(h)$ in the disk, whose inner accretion rate evolution is shown in Fig. 3. Top-hats are located at 0.94 – 1 (solid line) and 0.3 – 0.36 of $r_{\rm out}$ (dashed line) and the wide distribution, corresponding to $\Sigma(r) \propto r$, goes in $(0.1 - 1)\,r_{\rm out}$ (dotted line). The disk mass is the same in all cases and equals 1. The outer specific angular momentum $h_{\rm out} = 1$. The top-hat distributions are constructed using $\alpha_\Sigma = -1$. Parameter $l = 1/3$.

## 3.2. *The case of the disk with no central accretion and zero accretion rate at $r_{\rm out}$*

Condition $\partial F/\partial h = 0$ at $h = 0$ necessitates that all $A_i = 0$ in (14), which becomes for $t = 0$:

$$x^{-l}\,F(x, 0) = B_0 + \sum_{i=1}^{\infty} k_i^l\,B_i\,J_{-l}(k_i\,x)\,, \qquad (27)$$

where $k_i$ are the positive roots. In the previous section, the zero root contributed nothing to (16). Here the zero root provides a term like $(k_0\,x)^l J_{-l}(k_0\,x)$, which must contribute something, because the Bessel function $J_{-l}$ behaves as $\propto (k_0\,x)^{-l}$ in the vicinity of zero.

The method to find $B_i$ for $i \geq 1$ is analogous to that for $A_i$, since the Dini's series are convergent for the order of the Bessel function $> -1$ (Benedek & Panzone 1972; Guadalupe et al. 1993)[2]. We consider only non-integer $0 < l < 1$ and obtain

$$k_i^l\,B_i = 2\;x_1^{1-l}\,\frac{J_{-l}(k_i\,x_1)}{J_{-l}^2(k_i)}\;. \qquad (28)$$

It is known about the Dini's series of the negative order that an additional first term is to be added to the sum, if the equation defining roots $k_i$ has particular coefficients[3]. Just this

[2] The Hankel integral transform was also proved for the Bessel orders $> -1$ (?Betancor & Stempak 2001).

[3] For the usual form of writing the boundary condition for the Dini's series, $H\,J_\nu(z) + z J'_\nu(z)$=0, the the additional term appears if $H + \nu = 0$ (Watson 1944).

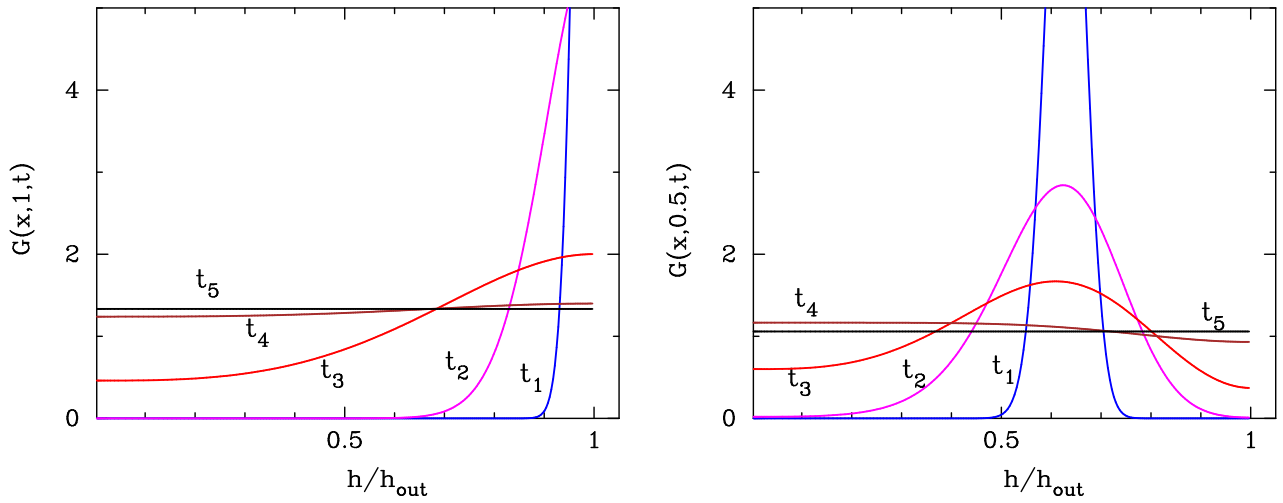


FIG. 5.— Green's function for the finite accretion disk with the zero accretion rate at the center at five moments of time $t_1 = 0.001$, $t_2 = 0.01$, $t_3 = 0.1$ $t_4 = 0.3$, $t_5 = 0.8$ (left) and $t_1 = 0.001$, $t_2 = 0.01$, $t_3 = 0.03$ $t_4 = 0.1$, $t_5 = 0.8$ (right). Initial spike is at position $x_s = (h/h_{\rm out})^{1/2l} = 1$ (left) and 0.5 (right). Constants $\kappa = 1$, $l = 1/3$, $t_{\rm vis} = 3/2$.

case occurs for the properly rewritten outer boundary condition (15):

$$l\, J_{-l}(k_i) + k_i\, J'_{-l}(k_i) = 0\,. \tag{29}$$

The additional term in the Dini's series is expressed as

$$B_0 = 2\,(1-l)\,x^{-l}\int\limits_0^1 z^{1-l}\,F(z,0)\,z^{-l}{\rm d}z\,, \tag{30}$$

where $z$ is a free variable (Watson 1944). Thus, adopting $F(z) = \delta(z - x_1)$, from (14) we obtain the Green's function for the equation of the non-stationary accretion with the zero inner accretion rate and the finite outer radius:

$$G(x,x_1,t) = 2\,(1-l)\,x_1^{1-2l} + \\ +\ 2\left(\frac{x}{x_1}\right)^l x_1 \sum_{i=1}^{\infty} e^{-t\,k_i^2\,\kappa^{-2}\,h_{\rm out}^{-1/l}}\,\frac{J_{-l}(k_i\,x_1)J_{-l}(k_i\,x)}{J^2_{-l}(k_i)}\,, \tag{31}$$

where $k_i$ are the positive roots of Eq. (29) and $x = (h/h_{\rm out})^{1/2l}$. Formulas (20) and (21) can be applied without changes.

This Green function is illustrated in Fig. 5. At the late stages, the accretion disks forget all information about the initial distribution of the viscous stresses. For the disks without accretion on to the center, the uniform distribution of $F$ develops, with its magnitude being proportional to the mass stored in the disk.

We take the derivative of (31) and obtain the Green function for the accretion rate:

$$G_{\dot M}(x,x_1,t) = \frac{x^{1-l}}{l}\sum_i e^{-t\,k_i^2\,\kappa^{-2}\,h_{\rm out}^{-1/l}}\,k_i\,\frac{J_{-l}(k_i\,x_1)\,J_{1-l}(k_i\,x)}{J^2_{-l}(k_i)}\,. \tag{32}$$

It approaches zero when $x \to 0$ for any time $t$. This corresponds to our boundary condition at the center: $\dot M = 0$. This disk, without sink of mass and additional mass supply, emits radiation even when it reaches the 'end' of its evolution, as the viscous heating (26) does not stop when the flow of matter ceases. If Fig. 6 its bolometric luminosity is plotted for the two initial positions of the ring (the details are given in the next subsection).

### 3.2.1. *The dead disk*

The stable configuration of the confined 'dead' disk (we adopt the name from the work by Syunyaev & Shakura 1977) has the following viscous angular momentum flux at each $r$:

$$F_{\rm d} \equiv F|_{t\to\infty} = \frac{4\,l\,(1-l)\,h_{\rm out}^{1-1/l}\,M_{\rm disk}}{\kappa^2} = 2\,(1-l)\,\frac{h_{\rm out}\,M_{\rm disk}}{t_{\rm vis}}\,, \tag{33}$$

where (24) is used and $t_{\rm vis} = 8\,l\,r_{\rm out}^{1/2l}\,(3\,\nu_0)^{-1}$ as before.

The total luminosity of the dead disk is a constant value $F_{\rm d}\,(\omega_{\rm in} - \omega_{\rm out})$. It can be obtained by the integration of (26) over the disk surface between $r_{\rm in}$ and $r_{\rm out}$. Unlikely to the case of the zero torque at $r = r_{\rm in}$, the late-time value of $F$ does not depend on the location at which condition $\dot M = 0$ is set and solely depends on the evolution at the large radii. This was shown for the infinite disks by Tanaka (2011). Value of $r_{\rm in}$ affects the limunosity only by a change in the size of the emitting surface. There is still a time-dependent correction obtained by Tanaka (2011) having an effect at early times $t < t_{\rm vis}(r_{\rm in}/r_{\rm out})^{2-b}$.

The dead-disk state has to end sometime, as the disk cannot receive infinitely the angular momentum from the central object. If the central star has a magnetosphere, its radius $r_{\rm mag}$ can be estimated from the equality of the viscous and magnetic torque at the magnetosphere boundary (LP74):

$$F(x\to 0) = \kappa_t\frac{\mu_\star^2}{r_{\rm mag}^3}\,, \tag{34}$$

where $\mu_\star$ is the magnetic dipole of the star, $\kappa_t$ is a dimensionless factor of order of unity (Lipunov 1992). Within some factor, this condition is equivalent to the equality of the gas and magnetic pressure at the inner disk boundary (Syunyaev & Shakura 1977). The accretion is inhibited if the inner disk radius, $r_{\rm mag}$, is greater than the corotation radius, because the drag exerted by the magnetic field is super-Keplerian:

$$r_{\rm cor} = \left(\frac{G\,M_\star}{\omega_\star^2}\right)^{1/3} = 1.7\times10^8\,P_\star^{2/3}\,M_{1.4}^{1/3}\ {\rm cm},$$

where $M_\star$, $\omega_\star$ and $P_\star$ are the mass, angular speed and period of the revolution of the central star. In the last expression the

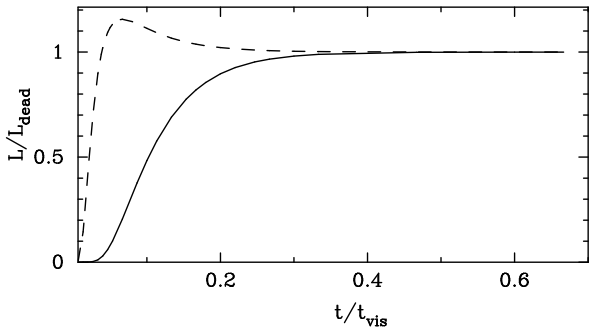


FIG. 6.— Variation of the luminosity of the disk with zero accretion rate through the inner radius normalized to value $L_{\rm dead} \equiv F_{\rm d}\,\omega_{\rm in}$. The disk starts from the outer radius (the solid line) or from $r = 0.5^{4l} \times r_{\rm out}$ (the dashed line), corresponding to the Green's functions in Fig. 5.

mass is normalized by 1.4 $M_\odot$. Thus we obtain for a final steady configuration

$$\frac{r_{\rm mag,d}}{r_{\rm cor}} \approx 1.4 \left(\frac{\kappa_{\rm t}}{1-l}\right)^{1/3} \frac{\mu_{30}^{2/3}\, t_{\rm vis,100}^{1/3}}{P_\star^{2/3}\, M_{1.4}^{1/2}\, M_{\rm disk,23}^{1/3}\, r_{\rm out,\odot}^{1/6}} .$$

The ratio can be rather close to unity. The normalizations are $10^{23}$ g for the disk mass, $10^{30}$ [G cm$^3$] for the magnetic dipole, 100 days for the viscous time, $R_\odot$ for the outer disk radius. Situation of $r_{\rm mag} \gtrsim r_{\rm cor}$ is studied by D'Angelo & Spruit (2010), who argue that no considerable expulsion of matter from the disk is expected in such regime, as contrasted to the propeller scenario. Using the magnetosphere radius as the inner disk radius, we find the steady disk luminosity:

$$L_{\rm dead} \approx 1.8\times10^{35}\, M_{\rm disk,23}^{3/2}\, M_{1.4}^{5/4}\, r_{\rm out,\odot}^{3/4}\, t_{\rm vis,100}^{-3/2}\, \mu_{30}^{-1}\, \kappa_{\rm t}^{-1/2} \ \ {\rm erg\ s^{-1}}$$

for $r_{\rm in} \ll r_{\rm out}$ from the both sides, for typical $l \sim 1/3$ (see Table 1). The upper limit on the luminosity of the disk with conserved mass is estimated when the inner radius equals the corotation radius:

$$L_{\rm dead,max} \approx 4.4\times10^{35}\, \mu_{30}^2\, P_\star^{-3}\, m_{1.4}^{-1} \ \ {\rm erg\ s^{-1}} .$$

The regime can be sustained for sufficiently strong magnetic dipole and fast rotation of the neutron star:

$$\mu_{30} P_\star^{-1} \gtrsim 0.63\, \sqrt{(1-l)/\kappa_{\rm t}}\, m_{1.4}^{3/4}\, M_{23}^{1/2}\, t_{\rm vis,100}^{-1/2}\, r_{\rm out,\odot}^{1/4} .$$

The flux of the angular momentum $F$ at small radii and the inner radius of the disk always manage to adjust themselves to the outer variations that proceed on longer viscous times. The steady value $F_{\rm d} \propto \nu_0\, r_{\rm out}^{b-3/2}$ could be low due to a degradation of $\nu_0$ in the outer disk with low luminosity. Then the normalized viscous time in the formulae above may be greater accordingly to $t_{\rm vis} \propto \nu_0$.

Luminosity during the spreading of the ring (Fig. 5) is calculated by integrating expression (26) over both surfaces of the disk confined between the outer and inner radius; it is plotted in Fig. 6. The inner radius of the disk is varying according to Eq. (34) and depends on the star's magnetic dipole. Its typical value $r_{\rm mag,d} = r_{\rm cor} \approx 2.4\times10^{-3} P_\star^{2/3}\, M_{1.4}^{1/3}\, R_\odot$.

The torque transfers the angular momentum of the central star to the disk and, via the disk, to the orbital motion of the binary. The corotation radius increases gradually and, eventually, accretion on the center begins (Syunyaev & Shakura 1977; D'Angelo & Spruit 2011). The characteristic brake time is the angular momentum of the star $2\pi I_\star/P_\star$ divided by the torque $F_{\rm d}$:

$$\frac{t_{\rm brake}}{t_{\rm vis}} \approx 10^4\, \frac{I_{\star,45}}{M_{1.4}^{1/2}\, r_{\rm out,\odot}^{1/2}\, P_\star\, M_{\rm disk,23}} ,$$

where $I_{\star,45} = I/10^{45}$ g cm$^2$ and a typical value of $l$ is substituted. If the mass of the disk grows due to the matter income, the braking time of the star shortens, while the magnetosphere radius decreases at the same time.

### 3.3. *The case of an arbitrary accretion rate at $r_{\rm out}$*

For a variable mass inflow $\dot M_{\rm out}(t)$ at the outer disk edge $r_{\rm out}$ the solution can be found by a procedure described in the Appendix B

$$F(x,t) = \int_0^1 \left(F_0(x_1) - \frac{x_1^{4l}}{2}\, h_{\rm out} \dot M_{\rm out}(t)\right) G(x,x_1,t)\,{\rm d}x_1 + \\ + \frac{h_{\rm out}}{2} \int_0^t\int_0^1 \left[\frac{8}{x_1^2}\left(\frac{l}{\kappa}\right)^2 \frac{\dot M_{\rm out}(\tau)}{h_{\rm out}^{1/l}} - \ddot M_{\rm out}(\tau)\right] x_1^{4l}\, G(x,x_1,t-\tau)\,{\rm d}x_1\,{\rm d}\tau + \\ + \frac{x^{4l}}{2}\, \dot M_{\rm out}(t)\, h_{\rm out} , \tag{35}$$

where $G(x,x_1,t)$ is given by (19) or (31). Substituting $G$ by $G_{\dot M}$ in the integrals above, and dividing the result by $h_{\rm out}$, we find the accretion rate in the disk $\dot M(x,t)$. We have tried the formula obtained in the numerous tests. In particular, it successfully reproduces the results obtained by numerical simulations of Mineshige (1994). The further details, however, are out of the scope of the present work.

## 4. THE ACCRETION DISK AT THE DECAY STAGE

We return now to the standard accretion disks with zero stress tensor at the center. For large $t$, the first term of the sum (22) dominates, and a single exponential dependence on time prevails:

$$G_{\dot M}(0,x_1,t)\Big|_{t>t_{\rm vis}} = \frac{k_1^l\, x_1^{1-l}}{2\, l\, \Gamma(l)}\, \frac{J_l(k_1\, x_1)}{J_l^2(k_1)}\, \exp\left(-\frac{t\, k_1^2}{2\, l\, t_{\rm vis}}\right) .$$

This corresponds to the well-known exponential dependence on time of the accretion rate in the disk with the time-independent viscosity $\nu$. The characteristic time of the exponential decay is

$$t_{\rm exp} = h_{\rm out}^{1/l}\, \frac{\kappa^2}{k_1^2} = \frac{16\, l^2}{3\, k_1^2}\, \frac{r_{\rm out}^2}{\nu_{\rm out}} , \tag{36}$$

where we use $\nu_{\rm out} = \nu_0\, r_{\rm out}^b$. In Table 1 we give locations $k_1$ of the first zeroes of equation (17) for several values of $l$. The table also lists the numerical factors in the expressions for the rise and decay time, (25) and (36).

At late times, the profile of $F(x,t)$ is self-similar, because $G(x,x_1,t\to\infty) \to x^l\, J_l(k_1,x)$. The distribution $\Sigma(r)$ is also self-similar. Actually, this profile develops already at the very beginning of the exponential decay. This is illustrated in Fig. 7 by the fact that the ratio of the inner accretion rate to the disk mass, which is the integral of the surface density, approaches a constant value that depends only on the form of the radial distribution. In Table 1, the values of the

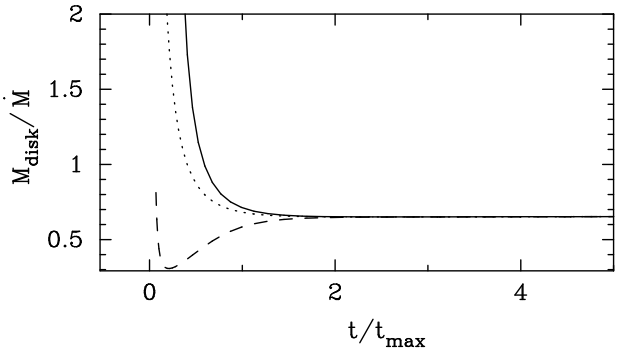


FIG. 7.— Ratio of the disk mass to the inner accretion rate vs. time normalized by the peak time. The constant value indicates a self-similar distribution in the disk has developed. The line styles and parameters are as in Fig. 3.

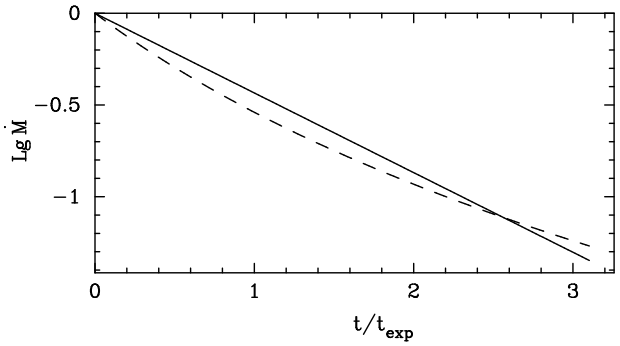


FIG. 8.— Relative variation of the accretion rate in two cases: $\nu = \nu_0\, r^b$ ($b = 3/4$, the solid line) and $\nu = \nu_0\, \Sigma^a\, r^b$ (Kramers' opacity, $a = 3/7$, $b = 15/14$, the dashed line). Disk parameters $r_{out}$ and $\nu_{out}$ are the same in the both models.

parameter $a_0 = \dot{M}_{in}\, h_{out}/F_{out}$ can be found. Parameter $a_0$ describes the self-similar profile of $F(h)$ and was calculated by Lipunova & Shakura (2000) for the non-stationary finite $\alpha$-disks. For the stationary disks with non-zero accretion rate, $a_0 = 1$.

What does the presence of this profile mean for the released energy in the disk? Using the energy balance equation for the optically thick disks, we obtain that at the outer radius $\sigma T_{\rm eff}^4 = (3/8\pi)\, \dot{M}_{in}\, \omega^2/a_0$, i.e. the outer ring luminosity is by factor $a_0 \approx 1.44$ less for the viscously evolving disk ($l = 2/5$) than in the case of the stationary disk. The factor $a_0(r) \approx 1.16$ for $r = 0.5 \times r_{out}$.

### 4.1. *Comparing with the $\alpha$-disks*

Let us now compare the finite-disk solution for the time-independent $\nu$ and that obtained for the turbulent viscosity in the general form $\nu = \nu_0\, \Sigma^a(t)\, r^b$. For the latter form of viscosity, Eq. (6) acquires the following view:

$$\frac{\partial F}{\partial t} = D\, \frac{F^m}{h^n}\, \frac{\partial^2 F}{\partial h^2}\,, \tag{37}$$

embracing a dimension constant

$$D = \frac{a+1}{2}\, (G\,M)^2 \left(\frac{3}{2}\, \frac{\nu_0}{(2\,\pi)^a\, (G\,M)^b}\right)^{1/(a+1)}\,,$$

and dimensionless parameters $m$ and $n$:

$$m = \frac{a}{a+1}\,, \qquad n = \frac{3\,a + 2 - 2\,b}{a+1}\,.$$

For a finite disk with such type of viscosity the inner accretion rate decays as a power law (Lipunova & Shakura 2000; Dubus et al. 2001):

$$\dot{M}(t) = \dot{M}(0)\, (1 + t/t_0)^{-1/m}\,, \tag{38}$$

where $\dot{M}(0)$ is the accretion rate at the time $t = 0$, which can be attributed to any moment of the decay stage. Eq. (37) describes the viscous evolution of the $\alpha$-disks.

The characteristic time of the solution $t_0 = h_{out}^{n+2}/(\lambda\, m\, D\, F_{out}^m(0))$, where $\lambda$ is a numerical constant that can be calculated for specific $a$ and $b$. Using the expression for $D$ and relation $F_{out} = 3\,\pi\, h_{out}\, \nu_{out}\, \Sigma_{out}$, we obtain

$$t_0 = \frac{4}{3\lambda\, a}\, \frac{r_{out}^2}{\nu_{out}(t=0)}\,. \tag{39}$$

For the $\alpha$-disk in the Kramers' regime of the opacity, parameters $a = 3/7$, $b = 15/14$, and $\lambda = 3.137$ (Lipunova & Shakura 2000) should be used in Eqs. (37)–(39). In this case, the dimensionless factor in (39) is close to unity. Value of $t_0$ depends on the choice of the zero time.

In the Shakura–Sunyaev disks, the viscous stress is proportional to the total pressure in the disk, and this proportionality is parametrized by the $\alpha$-parameter (Shakura 1973):

$$w_{r\varphi} = \alpha\, \rho\, {\rm v}_{\rm sound}^2\,.$$

Then the kinematic viscosity can be expressed using (5) as

$$\nu_{\rm t} = \frac{2}{3}\, \alpha\, \frac{{\rm v}_{\rm sound}^2}{\omega_{\rm k}} \tag{40}$$

or

$$\nu_{\rm t} = \frac{2}{3}\, \alpha\, \omega_{\rm k}\, r^2 \left(\frac{z_0}{r}\right)^2\,. \tag{41}$$

To approximate the viscous evolution of the $\alpha$-disk by the disk with steady viscosity, one has to estimate the appropriate parameter $b$ for Eq. (8) and (9). This can be effectively done using the relation $\nu_{\rm t} \propto r^{1/2}\, (z_0/r)^2 \propto r^b$. The solution for the stationary pressure-dominated stationary regions (Shakura & Sunyaev 1973) gives the relative half-thickness $z_0/r \propto r^{1/8}$, consequently, $b \simeq 3/4$ or $l \simeq 2/5$ in (9), for the free-free opacity regime. Table 1 lists the parameters approximating in a similar way the standard $\alpha$-disk with the Thomson opacity and the 'dead' disks models (Syunyaev & Shakura 1977).

In Fig. 8 the two laws are plotted: exponential $\propto \exp(-t/t_{\rm exp})$ for $l = 2/5$ and power-law (38) for $m = 3/10$. Viscosity at the outer radius and the outer radius itself are the same. If applied to the real bursts during the time spans of order of $\sim t_{\rm exp}$, the models cannot be easily discriminated (this was also pointed at by Dubus et al. 2001). This fact provides a possibility to estimate $\alpha$ using the $e$-folding time of the light curve. In the next Section, we show how it could be done using the observations of the disks in X-ray novae, whose light curves in many cases show exponential decays.

## 5. THE BURST LIGHT CURVES OF X-RAY NOVAE

In the X-ray novae, binary systems with a compact star and, typically, a less-than-solar-mass optical star, transient outbursts are thought to originate due to a dwarf nova-type instability (e.g., Lasota 2001). The temperature rises in a portion of the 'cold' neutral disk, which becomes ionized, and the viscosity $\nu$ rises. Moreover, the turbulent parameter $\alpha$ changes from $\alpha_{\rm cold}$ to higher $\alpha_{\rm hot}$. The heating front moves outward from some ignition radius with the speed $V_{\rm front} \sim \alpha_{\rm hot}\, {\rm v}_{\rm sound}$.

TABLE 1
PARAMETERS OF THE GREEN'S FUNCTIONS FOR TWO TYPES OF INNER BOUNDARY CONDITION.

| $b$ (1) | $l$ (2) | $k_1$ (3) | $t^{\infty}_{\max}(r_s^2/\nu_s)^{-1}$ (4) | $t_{\exp}(r^2_{\rm out}/\nu_{\rm out})^{-1}$ (5) | $a_0$ (6) | Comment (7) |
|---|---|---|---|---|---|---|
| 0 | 1/4 | 1.0585 | 1/15 | 0.298 | 1.267 | constant $\nu$ |
| 1/2 | 1/3 | 1.2430 | 1/9 | 0.383 | 1.363 | $\alpha-$disks with constant $h/r$; $\beta-$disks |
| 3/5 | 5/14 | 1.2927 | 0.125 | 0.407 | 1.392 | $\alpha-$disks, Thomson opacity ($a_0 = 1.376$[1]) |
| 3/4 | 2/5 | 1.3793 | 0.152 | 0.449 | 1.444 | $\alpha-$disks, Kramers' opacity ($a_0 = 1.430$[1]) |
| 1 | 1/2 | 1.5708 | 2/9 | 0.540 | 1.571 | $F(h) \propto \sin((\pi/2)\, h/h_{\rm out})$ |
| 2 | $\infty$ | — | — | — | — | $t_{\rm visc}$ does not depend on $r$ |
| 2/5 | 5/16 | 3.4045 | 0.189 | — | 0 | dead $\alpha-$disks, Thomson opacity |
| 3/5 | 5/14 | 3.3425 | 0.265 | — | 0 | dead $\alpha-$disks, Kramers' opacity |

NOTE. — Columns are as follows: (1) The index of the radial dependence of $\nu$; (2) $l$ defined by (12); (3) The first zero of equations (17) and (29), in the upper and lower part, respectively; (4) The dimensionless factor in (25) (the upper part) and the one in a similar formula derived by LP74 for the time of maximum $F$ in the disk without central accretion (the lower part of the Table); (5) The dimensionless factor in (36); (6) Parameter describing the self-similar radial profile, $a_0 = \dot{M}_{\rm in}\, h_{\rm out}/F_{\rm out}$; (7) Note on the applicability. The opacity law is indicated for the $\alpha$-disks. The applicability of parameters is approximate for the $\alpha$-disk. Refs: [1]Lipunova & Shakura (2000).

It stops at a radius, where the surface density of the disk is too low to sustain the stable (on the thermal time-scale) hot state (Meyer 1984; Menou et al. 2000; Dubus et al. 2001; Lasota 2001).

In the dwarf novae, the hot state accretion is quenched swiftly (comparing to the viscous time) by the matter returning to the cold state. It was suggested that in the X-ray novae the illumination from the center has a stabilizing effect on the outer disk, keeping the temperatures above the hydrogen ionization temperature (Meyer & Meyer-Hofmeister 1984; Chen et al. 1993). King & Ritter (1998) propose that in order for the disk to undergo the viscous evolution an intensive irradiation must be included.

A canonical light curve of an X-ray nova is described as a FRED (Chen et al. 1997). Theoretically, if the disk is truncated from outside, a steeply decaying light curve is produced (King & Ritter 1998; Lipunova & Shakura 2000; Wood et al. 2001). The main property is that the disk does not expand infinitely, which is a consequence of its being in a binary system, and its radius does not change on a viscous time scale. Scenario by King & Ritter (1998) produces exponential decays due to the steadiness of the parameter $\nu$ in time. More realistic temporal dependence of $\nu$ leads to a steep power-law decay (Lipunova & Shakura 2000; Dubus et al. 2001), which is close to an exponential one during few viscous times (see the previous Section).

The possibility to model the X-ray novae bursts, which have the FRED profile, by the viscously evolving disk with the steady viscosity and after a descrete mass-transfer event, was shown by Wood et al. (2001) (see also the modeling in Sturner & Shrader 2005). If a burst is due to an instability affecting a slab of matter extended along the radii, the Green's function obtained in the present work should be used. Effectively, after a heating front has passed, the dwarf-nova type instability leads to some distribution of the hot-ionized matter with high viscosity. In the most trivial case, when the bulk mass is concentrated near $r_{\rm out}$, the evolution of the disk approaches the one found by Wood et al. (2001).

Let us compare the typical time of the heating front propagation $r/V_{\rm front}$ and the time $t_{\max}$ it takes the inner accretion rate to peak, which is of order of $t^{\infty}_{\max}$ (see (25) and Fig. 2). Relating $\alpha$ and $\nu$ by (40), we obtain:

$$\frac{t_{\rm front}}{t_{\max}} = \frac{l+1}{2\,l^2}\,\sqrt{\frac{r_{\rm s}\,{\rm v}^2_{\rm sound}}{G\,M}} \sim 0.1\sqrt{\frac{T_4\, r_{11}}{\mu\, m_x}},$$

where the gas temperature is normalized by $10^4$ K, central star mass by a solar mass, and radius by $10^{11}$ cm, $\mu$ is the molecular weight of the hot matter. Radius $r_s$ is the characteristic radius where the bulk mass resides at the beginning of an outburst. This ratio indicates that we are safe to model an X-ray nova outburst at time $\sim t_{\max}$ using the Green's function obtained.

If one assumes the commonly suggested surface density distribution in the quiescent state in the X-ray novae, $\Sigma \propto r$ (Lasota 2001), then, as it is shown in Fig. 3, after the peak of the burst, the only important parameters are the disk mass and the outer radius. For such density distribution, the bulk mass of the disk resides close to the outer radius. As we show in Sect. 4, already at the maximum of an outburst the disk acquires the self-similar radial distribution, which is not dependent on the initial distribution of matter. The necessary condition for this is that the bulk mass of the viscously evolving disk is located near the outer radius. This is consistent with the absence of a power-law interval before the exponential decline on the the light curves of the X-ray novae that show the FRED behaviour.

Eqs. (25) and (36) yield the ratio $t_{\exp}/t_{\max}$ taking into account that $t_{\max}$ is very close to $t^{\infty}_{\max}$ for $r_{\rm s} \sim r_{\rm out}$. The value of $t_{\max}/t^{\infty}_{\max}$ is depicted in Fig. 2, where $t_{\max}$ is the peak time for the finite disk. For $l = 2/5$ (see Table 1) we obtain $t_{\exp}/t_{\max} \approx 3$. This provides a rough test whether the particular light curve is produced by the viscously evolving disk made of hot ionized matter and with approximately constant outer radius.

The viscous-disk relation $t_{\rm rise} \approx 0.15\, r^2_{\rm out}/\nu_{\rm out}$ for the hot-disks with the Kramers' opacity in the outer parts leads to a conclusion that to obtain a secondary maximum on the X-ray light curve of an X-ray nova, the disk has to provide an extra mass input at the radius that is determined by the time of the input. The secondary maximuma are usually observed around $(1-2)\, t_{\exp}$ after the peak. If the extra mass input happens at the time of the burst maximum then it should happen at least at a radius about $2.4\, r_{\rm out}$ (from $t_{\exp}/t_{\rm rise} \sim 3$ and $\nu \propto r^{3/4}$), without

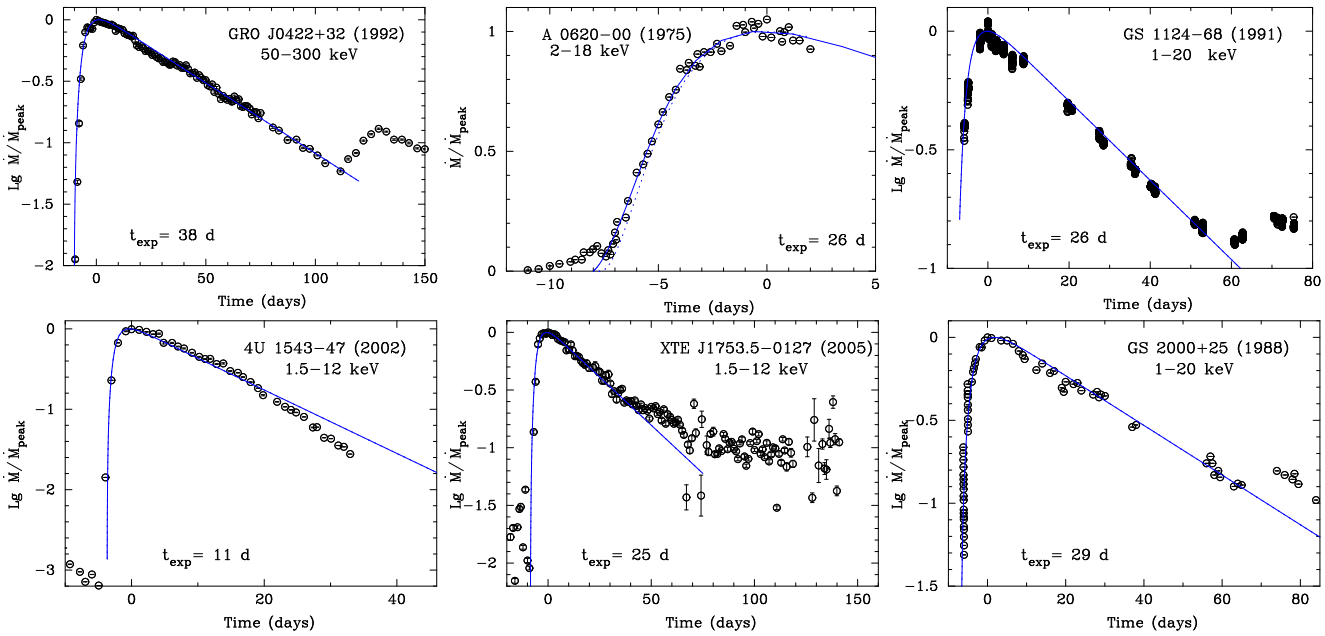


FIG. 9.— The peak-normalized light curves of GRO J0422+32 in 1992, A 0620-00 in 1975, GS 1124-68 in 1991, GS 2000+25 in 1998 (as collected in Chen et al. 1997) and 4U 1543-47 in 2002 and XTE J1753.5-0127 in 2005 (the quick-look results provided by the ASM/RXTE team). The energy bands of the X-ray data are indicated in the plots. The model curves are the peak-normalized accretion rate, calculated by (21) using $t_{\rm exp}$ indicated for each burst, and $l = 2/5$. The initial surface density distribution $\Sigma \propto r$, and the inner radius of the initial hot zone is $0.01 \times r_{\rm out}$. Note the different axis scale for A 0620-00, for which two different models are plotted, with the initial inner radius at $0.001 \times r_{\rm out}$ (solid line) and $0.3 \times r_{\rm out}$ (dotted line).

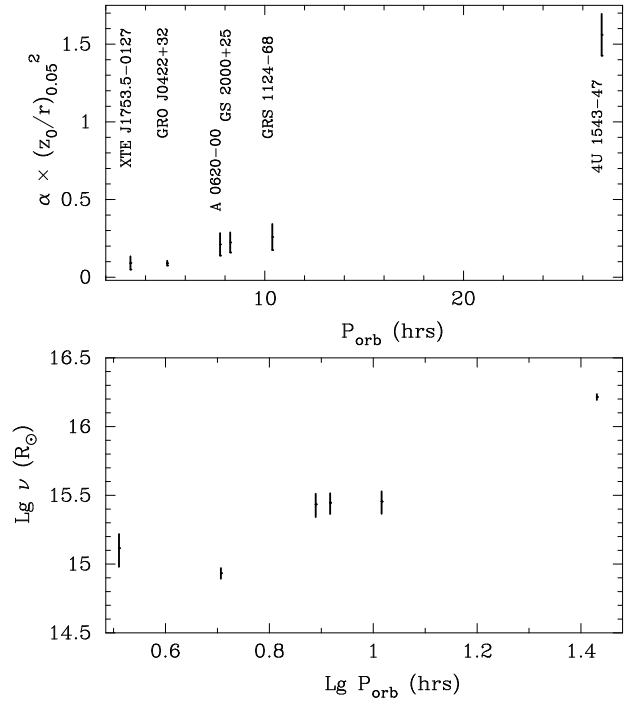


FIG. 10.— Top panel: estimates for the turbulent parameter $\alpha$ times the square relative half-thickness of the disk at $r_{\rm out}$ for the six bursts of X-ray novae. Lower panel: corresponding estimates of the viscosity parameter $\nu$ at $r = \mathrm{R}_\odot$.

mass input from the intermediate radii. Another possibility is that the secondary maximum is triggered later after the peak and then it can happen at a radius $\sim r_{\rm out}$ (as in the model of Ertan & Alpar 2002).

If an X-ray nova has the viscously evolving accretion disk with constant $r_{\rm out}$ during the interval of the 'exponential decay' (usually, first $\sim$ 50 days after the peak), we can infer the value of the turbulent parameter $\alpha$, using the closeness of the model with steady visosity and the $\alpha$-disk. As the irradiation, which provides the steadiness of the hot zone outer radius, does not change the vertical structure of the disk (Dubus et al. 1999), we can adopt $l = 2/5$ applicable for the hot ionized standard $\alpha$-disks. Combining Eqs. (36) and (41), we get

$$\alpha \approx 0.15 \left(\frac{r_{\rm out}}{2\,R_\odot}\right)^{3/2} \left(\frac{z_0/r_{\rm out}}{0.05}\right)^{-2} \left(\frac{M}{10\,M_\odot}\right)^{-1/2} \left(\frac{t_{\rm exp}}{30^{\rm d}}\right)^{-1} , \quad (42)$$

which relates the $\alpha$-parameter to the observed $t_{\rm exp}$, the $e$-folding time of the bolometric luminosity or the inner accretion rate. The last formula resembles quite a few others found in the literature. Similarly, the relation of $\alpha$ to the half-thickness of the disk cannot be eluded. However, an advatage is that (42) contains the e-folding time which can be inferred quite accurately from observations.

We have sampled six FRED light curves in different X-ray novae (Fig. 9) and fitted them with the steady-$\nu$ viscously-evolving disk model. For particular values of $t_{\rm exp}$, the model curves agree well with the peak-normalized count-rates before the second maximum, which is observed in most of the cases. For A 0620-00, we use the value of $t_{\rm exp}$, estimated by Chen et al. (1997) from the 3−8 keV light curve during the decline. Variation of the initial inner radius of the hot zone leads to slight changes of the model curve for the particular initial distribution of $\Sigma(r)$, as can be seen in the panel for A 0620-00.

In Fig. 10 we plot the estimates for $\alpha$-parameter times the normalized square of the relative half-thikness at the outer radius of the disk. Theses estimates are obtained using (42) with the values $t_{\rm exp}$ indicated in Fig. 9. In the lower panel, the viscosity $\nu$ is plotted, found accordingly to (36). As $\nu$ is not constant over radius, we choose to present its value at the same radius $\mathrm{R}_\odot$ for all cases. The considered X-ray novae have known orbital periods. The masses of the primary and secondary components, mass ratios are from Charles & Coe

(2006). For black hole candidate XTE J1753.5-0127 with $P_{\rm orb} = 3.24$ hr (Zurita et al. 2008) we set rather arbitrarily $M = 3 - 15$ M$_\odot$ and $M_{\rm sec} = 0.2 - 1.2$ M$_\odot$. The Roche lobes $R_{\rm RL}$ are calculated using the formula by Eggleton (1983), and $r_{\rm out}/R_{\rm RL} = 0.88 \pm 0.02$. The vertical barrs in Fig. 10 reflect the errors related to the uncertainties of the binary parameters and do not take into account uncertainty of $t_{\rm exp}$.

Suleimanov et al. (2007) give the half-thickness of the outer parts for the stationary $\alpha$-disks when the hydrogen is completely ionized:

$$z_0/r \approx 0.05\,(M/\mathrm{M}_\odot)^{-3/8}\,\dot{M}_{17}^{3/20}\,r_{10}^{1/8}\,\alpha^{-1/10}\,,$$

with the parameters' normalizations equal to $10^{17}\,\mathrm{g\,s^{-1}}$ and $10^{10}$ cm. It can be rewritten for the factor in Fig. 10 as follows

$$\left(\frac{z_0/r}{0.05}\right)^2 \approx 1 \times \left(\frac{M}{10\,\mathrm{M}_\odot}\right)^{-9/20} \left(\frac{\dot{M}}{0.1\,\dot{M}_{\rm cr}}\right)^{3/10} \left(\frac{r_{\rm out}}{\mathrm{R}_\odot}\right)^{1/4} \alpha_{0.1}^{-1/5}\,,$$

where $\alpha$ is normalized to 0.1 and $\dot{M}_{\rm cr}$ is the conventional rate of accretion producing the critical luminosity: $0.1\,\dot{M}_{\rm cr}\,c^2 = 1.3 \times 10^{38} (M/\mathrm{M}_\odot)\ \mathrm{erg\,s^{-1}}$. For the black hole masses in the range $3 - 15$ M$_\odot$, accretion rates in $(0.01 - 0.5)\,\dot{M}_{\rm cr}$, $\alpha$ in $0.1-0.5$, and $r_{\rm out}$ in $1-3$ R$_\odot$, the above factor changes between extremes $\sim 0.3$ and $\sim 3.8$. For 4U 1543-47 with parameters $\dot{M}/\dot{M}_{\rm cr} \approx 0.25$ (Wu et al. 2010), $M = 9.4$ M$_\odot$ (Charles & Coe 2006), $r_{\rm out} = 4.5$ R$_\odot$ $= 0.9 \times R_{\rm RL}$ and $\alpha = 0.2$ one obtains the factor $(z_0/r/0.05)^2 \approx 1.8$. It follows from Fig. 10 that $\alpha$ can be less than 1 in this case, but this is still not a self-consistent value. Apparently, the disk in this longer-period X-ray nova was not entierly involved in the viscous evolution that produced the FRED light curve in 2002. Levels of $\alpha$ of the other five bursts (Fig. 10, the upper panel) agree with the estimates for the fully ionized, time-dependent accretion disks obtained by various approaches in X-ray and dwarf novae (King et al. 2007; Suleimanov et al. 2008; Kotko & Lasota 2012), in the decretion disks of Be stars (Carciofi et al. 2012).

The values of $t_{\rm exp}$, indicated in Fig. 9, are to be considered with caution. Note that the observed light curves are limited to an energy band. Spectral modeling might be required in many cases to obtain accurate $t_{\rm exp}$. If an X-ray nova during the burst is in the *high/soft* state, when the disk emission dominates the spectrum, the spectral modeling can provide $T_{\rm in}(t) \propto \dot{M}_{\rm in}^{1/4}(t)$ in a straightforward way. We expect $t_{\rm exp}$ not to alter by a factor larger than 2 for the X-ray flux dominated by the disk (preliminary resluts for 2-10 keV).

On the other hand, some X-ray novae bursts proceed entirely in the *low/hard state*, such as the burst of XTE J1753.5.-0127 (Miller & Rykoff 2007). Still, the form of the corresponding X-ray light curves is informatve. Even if the optically thick disk does not reach the innermost orbits, it is very probable that the radiated energy is proportional to the accretion rate, because the released potential gravitational energy is the ultimate source to power the source. Second, the innermost disk peculiarities do not influence the behavior of $\dot{M}(t)$ as the latter is defined by the process of the viscous matter redistribution in the outer disk.

## 6. DISCUSSION

Equation (6) is written without the tidal-stress term, following the proposition that it should be negligible everywhere in the disk, except in a thin ring near the tidal truncation radius (Ichikawa & Osaki 1994). According to Pringle (1991), effects near the tidal-torque radius can be approximated with an effective boundary condition $\dot{M} = 0$. Numerical models confirm that most of the tidal torque is applied in a narrow region at the edge of the disk, where perturbations become non-linear and strong spiral shocks appear (Pringle 1991; Ichikawa & Osaki 1994; Hameury & Lasota 2005, and references therein). As Smak (2000) notes, in the case of dwarf novae, during outbursts, the observed values of the outer radius appear to be approximately consistent with the theoretical predictions. Hameury & Lasota (2005) argue that the action of the tidal torques are important also well inside the tidal radius. They notice at the same time that observations do not allow discriminating between the rapidly growing and smoother tidal stresses, as the model light curves are not strongly affected.

The tidal radius for all mass ratios can be approximated as $0.88 \pm 0.02$ of the average Roche lobe radius of a given component in circular binaries (Papaloizou & Pringle 1977). The disk can extend beyond this radius due to the high inclination of the binary orbit (Okazaki 2007). Effects of the high eccentricity of the binary orbit on the disk truncation radius have been studied by various methods (e.g., Artymowicz & Lubow 1994; Pichardo et al. 2005; Okazaki 2007).

The gravitational influence of the secondary on the disk in a binary system leads to a number of interactions, non-resonant (or tidal) and resonant, any of those transferring angular momentum from the disk to the binary (Artymowicz & Lubow 1994). The tidal distortions generally lead to the truncation of the disk, whereas the resonances of different strength impact or do not the disk structure, depending on their growth rate and other conditions (Whitehurst & King 1991; Ogilvie 2002). An example of a resonance action is the debated explanation of the superhamps in SU UMa stars (see, e.g. Lubow 1991; Kornet & Rozyczka 2000; Hameury & Lasota 2005).

In our mathematical set-up, we have presumed a fixed outer radius of the disk without going into details of its actual value. Thus the model is appplicable to the coplanar disks in low-eccentricity binaries. The outer radius of the disk can also change due to intrinsic processes. Reproducing the whole evolutionary cycles of the dwarf novae and X-ray novae, Smak (2000), Dubus et al. (2001) should have taken into account the variations of the outer disk radius, but these changes are significant during the time spans much greater than the viscous times.

## 7. SUMMARY

Under some astrophysical conditions, viscously evolving disks formed in binary systems are effectively truncated from outside. In the present work, we use the method proposed by Lüst (1952) to find the Green's functions for the linear viscous evolution equation for the disk with the finite outer radius. Green's functions are obtained for the viscous angular momentum flux $F$ and the accretion rate $\dot{M}$. Two inner boundary conditions at the zero coordinate are considered. They correspond to the accreting disks and to the disks with no mass sink at the center. The Green's functions allow one to compute $\Sigma(r,t)$ and $\dot{M}(r,t)$ for arbitrary initial surface density profiles that develop into self-similar distributions on sufficiently long time scale. The analytic formula to calculate the disk evolution with the variable outer mass inflow is derived. A solution, which can be found with the use of the Green's function, has the properties defined by the main equation of the viscous evolution and thus provides the basic description of the transient phenomena in the viscous disk.

The Green's functions are found in the form of quickly

converging series and can be easily reproduced with standard computer methods. The C-code written for the case of the accreting disc with the use of the GNU Scientific Library[4] can be downloaded[5].

We present the relations between the rising time, $e$-folding time, and disk viscosity. For six bursts in the X-ray novae, which are of FRED type, we show that the model describes well the peak-normalized light curves before the second maximum. This favors the mainly viscous nature of their evolution during this period and enables us to obtain an estimate of viscosity $\nu$, which depends on the outer disk radius.

The models with time-independent viscosity are shown to approximate well the evolution of $\alpha$-disks during time intervals comparable to the viscous time. Consequently, estimates of the $\alpha$ parameter may be derived for the disks in the binaries with known period and masses. These estimates rely on the relative half-thickness of the disk at the outer radius. The estimates of $\alpha$ for the five short-period X-ray novae outbursts, GRO J0422+32 in 1992, A 0620-00 in 1975, GS 1124-68 in 1991, GS 2000+25 in 1998, and XTE J1753.5-0127 in 2005, are in line with the values estimated so far for the hot viscous disks (King et al. 2007; Suleimanov et al. 2008; Kotko & Lasota 2012).

Another Green's fucntion is found for the disk that has zero accretion rate at the inner radius and acquires angular momentum from the central star. In the steady state, the mass of the disk cannot be very high and the disk has low luminosity. It radiates most of the rotational power transferred from the central star. This disk works as a gear transmitting the angular momentum of the central star to the orbital motion. The 'dead' stage is ended by an abrupt fall or trickle of the matter on to the star after the centrifugal barrier has moved close enough or beyond the magnetosphere's radius.


## ACKNOWLEDGEMENTS

The author is grateful to N. I. Shakura, K. Stempak, J. L. Varona, M. Perez and the anonymous referee for useful comments. The work is supported by the Russian Science Foundation (grant 14-12-00146).


## APPENDIX

## INFINITE DISKS: GREEN'S FUNCTION AND BASIC RELATIONS

Green's function for the infinite disk, obtained by LP74, can be written in the dimensionless form with our designations (c.f. formula (19)) as follows:

$$G^{\infty}(x, x_1, t) = \frac{\kappa^2\, h_{\rm c}^{1/l}\, x^l\, x_1^{1-l}}{2\,t} \exp\left(-\frac{x_1^2 + x^2}{4t}\,\kappa^2\, h_{\rm c}^{1/l}\right) I_l\left(\frac{x\,x_1}{2t}\,\kappa^2\, h_{\rm c}^{1/l}\right),$$

where $I_l$ is the modified Bessel function of the first kind, $x = (h/h_{\rm c})^{1/2l}$, $h_{\rm c}$ is some characteristic value of the specific angular momentum, which we use instead of $h_{\rm out}$.

To find the physical distribution of $F(x, t)$ in the course of the evolution of the initial narrow ring of matter, initially located at the coordinate $x_s$, one takes the integral of $F(x_1, 0)$ (24) with the kernel $G^{\infty}$ on the interval $x_1 \in [0, \infty]$:

$$F(x, t) = \frac{M_{\rm disk}\, h_{\rm c}\, l\, (x\, x_s)^l}{t}\, \exp\left(-\frac{x_s^2 + x^2}{4t}\,\kappa^2\, h_{\rm c}^{1/l}\right) I_l\left(\frac{x\, x_s}{2t}\,\kappa^2\, h_{\rm c}^{1/l}\right),$$

where $M_{\rm disk}$ is the initial mass of the ring.

The accretion rate at the center can be found from $\dot{M}_{\rm in} = \partial F/\partial h|_{h\to 0}$ (see (21)). One finds

$$\dot{M}_{\rm in}(t) = \frac{x^{1-2l}}{2\,l\,h_{\rm c}}\,\frac{\partial F}{\partial x}\Big|_{x\to 0} = \frac{M_{\rm disk}\tau_e^l}{\Gamma(l)}\,\frac{e^{-\tau_e/t}}{t^{1+l}},$$

or

$$\dot{M}_{\rm in}(t) = \dot{M}^{\infty}_{\rm in,\,peak}\left(\frac{\tau_{\rm pl}}{t}\right)^{1+l} e^{-\tau_e/t},$$

where the typical times $\tau_{\rm pl}$ and $\tau_e$ are introduced,

$$\tau_e = \frac{\kappa^2\, h_{\rm s}^{1/l}}{4} = \frac{1+l}{e}\,\tau_{\rm pl}\,.$$

We find that the accretion rate peaks at the time (25) $t^{\infty}_{\rm max} = \tau_e/(1+l)$ with the value

$$\dot{M}^{\infty}_{\rm in,\,peak} = \frac{M_{\rm disk}}{t^{\infty}_{\rm max}}\,\frac{(1+l)^l}{e^{1+l}\,\Gamma(l)}\,. \tag{A1}$$

## SOLUTION FOR THE CASE WITH VARIABLE ACCRETION RATE AT THE OUTER EDGE OF THE DISK

For infinite disks, see Metzger et al. (2012) and Shen & Matzner (2014), who have obtained the Green's function solution to the viscous evolution of a disk with mass sources/sinks, which are distributed in a fashion along the disk radius.

[4] http://www.gnu.org/software/gsl/

[5] http://xray.sai.msu.ru/~galja/lindisk.tgz

We have the following problem with the inhomogeneous boundary and initial conditions:

$$\begin{aligned} &\frac{\partial^2 F}{\partial h^2} = \frac{1}{4}\left(\frac{\kappa}{l}\right)^2 h^{1/l-2}\,\frac{\partial F}{\partial t} \\ &\partial F/\partial h|_{h=h_{\rm out}} = \dot{M}_{\rm out}(t) \\ &F\,|_{t=0} = F_0(h)\,. \end{aligned} \tag{B1}$$

Let us substitute function $F(h)$ by a function $\tilde{F}(h)$ using the relation

$$F(h) = \tilde{F}(h) + \frac{h^2}{2\,h_{\rm out}}\,\dot{M}_{\rm out}(t)\,. \tag{B2}$$

This substitution is used, for example, to solve the problem of finding the temperature distribution in a cylinder, on a surface of which a thermal flux is defined (Bogolyubov & Kravtsov 1998). For the new $\tilde{F}(h)$ the problem is the following:

$$\begin{aligned} &\frac{\partial \tilde{F}}{\partial t} = 4\left(\frac{l}{\kappa}\right)^2 h^{2-1/l}\,\frac{\partial^2 \tilde{F}}{\partial h^2} + \Phi(h,t)\,, \\ &\partial \tilde{F}/\partial h|_{h=h_{\rm out}} = 0\,, \\ &\tilde{F}\,|_{t=0} \equiv \tilde{F}_0(h) = F_0(h) - \frac{h^2}{2\,h_{\rm out}}\,\dot{M}_{\rm out}(t=0)\,, \end{aligned} \tag{B3}$$

where

$$\Phi(h,t) \equiv 4\left(\frac{l}{\kappa}\right)^2 \frac{h^{2-1/l}\,\dot{M}_{\rm out}}{h_{\rm out}} - \frac{h^2}{2\,h_{\rm out}}\,\frac{{\rm d}\dot{M}_{\rm out}}{{\rm d}t}\,.$$

The corresponding Sturm–Liouville problem with a free variable $\xi = h/h_{\rm out}$ is investigated in Sect. 3: it consists of Eq. (13)

$$\frac{\partial^2 f_i(\xi)}{\partial \xi^2} + \frac{1}{4}\,s_i\left(\frac{\kappa}{l}\right)^2 h_{\rm out}^{1/l}\,\xi^{1/l-2}\,f_i(\xi) = 0\,, \tag{B4}$$

where $s_i$ or $k_i = s_i^2\kappa^2 h_{\rm out}^{1/l}$ plays a role of an eigenvalue, and the boundary condition $\partial f_i(\xi)/\partial\xi = 0$ at $\xi = \xi_{\rm out}$. Changing to the free variable $x = \xi^{1/2l} = (h/h_{\rm out})^{1/2l}$, we can write for a non-integer $l$

$$f_i(x) = (k_i x)^l\,[\tilde{A}_i\,J_l(k_i\,x) + \tilde{B}_i\,J_{-l}(k_i\,x)]\,,$$

where $\tilde{A}_i$ and $\tilde{B}_i$ depend on the inner-boundary condition. According to the Steklov theorem, the solution to (B3) can be obtained in the form:

$$\tilde{F}(h,t) = \sum_{n=1}^{\infty} u_i(t)\,f_i(x)\,, \tag{B5}$$

where coefficients $u_i(t)$ are to be found from the inhomogeneous first-order differential equation over $t$. Let us substitute (B5) into (B4) and (B3), multiply by $f_n(x)$ and integrate over $x$ from 0 to 1, using the orthogonality property of the eigenfunctions. We arrive at

$$\begin{aligned} &\frac{\partial u_n(t)}{\partial t} + s_i\,u_n(t) = \Phi_n(t)\,, \\ &u_n\,|_{t=0} = \phi_n\,, \end{aligned} \tag{B6}$$

with designations

$$\phi_n = \int_0^1 \tilde{F}_0(x)\,f_n(x){\rm d}x\Big/\|f_n\|^2;\ \Phi_n(t) = \int_0^1 \Phi(h(x),t)\,f_n(x){\rm d}x\Big/\|f_n\|^2\,, \tag{B7}$$

where $\|f_n\|^2$ is the norm of eigenfunction $f_n$. Solution to (B6) is as follows

$$u_i(t) = \phi_i\,e^{-s_i\,t} + \int_0^t \Phi_i(\tau)\,e^{-s_i\,(t-\tau)}\,{\rm d}\tau\,.$$

Let us write down the solution to (B3) for the case $\dot{M}_{\rm out} = 0$, that is, $\Phi(h,t) = 0$:

$$\tilde{F}(x,t) = \sum_{i=1}^{\infty} \phi_i\,e^{-s_i\,t}\,f_i(x)\,.$$

The last expression is equivalent to (14). In Sect. 3, we find the coefficients $\phi_i = A_i$ and $B_i$ for the Dirac delta function as the initial condition and express $F(x,t)$ using the Green's function. In the analogy, the solution to the problem with $\Phi(h,t) \neq 0$ has the view

$$\tilde{F}(x,t) = \int_0^1 \tilde{F}_0(x_1)\, G(x,x_1,t)\,\mathrm{d}x_1 \; + \int_0^t\int_0^1 \Phi(x_1,\tau)\, G(x,x_1,t-\tau)\,\mathrm{d}x_1\,\mathrm{d}\tau\,, \tag{B8}$$

where $G(x,x_1,t)$ is given by (19) or (31).

Substituting (B8) into (B2) and using functions $\tilde{F}_0$ and $\Phi$ from (B3), we finally arrive at (35). The coordinate integral in its second term can be taken analytically; it involves the Lommel functions and can be tabulated beforehand for the particular values of $l$ and $k_i$ for the sake of the computational efficiency. The second term of (35) for $B_i = 0$ can be expressed as:

$$h_{\rm out}\, x^l \sum_i J_l(k_i\, x) \int_0^t \exp\!\left(-\frac{t-\tau}{t_{\rm vis}}\,\frac{k_i^2}{2l}\right)\left[4\,l\,L_1\,\frac{\dot{M}_{\rm out}(\tau)}{t_{\rm vis}} - L_2\,\ddot{M}_{\rm out}(\tau)\right]\mathrm{d}\tau\,, \tag{B9}$$

where

$$L_1 = \int_0^1 x_1^{3\,l-1}\, J_l(k_i\,x_1)\,\mathrm{d}x_1 \Big/ J_l^2(k_i);\; L_2 = \int_0^1 x_1^{3\,l+1}\, J_l(k_i\,x_1)\,\mathrm{d}x_1 \Big/ J_l^2(k_i)\,. \tag{B10}$$

## REFERENCES


Artymowicz, P., & Lubow, S. H. 1994, ApJ, 421, 651
Barenblatt, G. I. 1996, Scaling, Self-similarity, and Intermediate Asymptotics: Dimensional Analysis and Intermediate Asymptotics, Cambridge Texts in Applied Mathematics, Cambridge University Press
Benedek, A., & Panzone, R. 1972, Revista de la Unión Matemática Argentina, 26, 42
Betancor, J. J., & Stempak, K. 2001, Tohoku Mathematical Journal, 53, 109
Bogolyubov, A. N., & Kravtsov, V. V. 1998, Problems of Mathematical Physics, ed. A. G. Sveshnikov, Moscow State University Press
Cannizzo, J. K., Lee, H. M., & Goodman, J. 1990, ApJ, 351, 38
Carciofi, A. C., Bjorkman, J. E., Otero, S. A., Okazaki, A. T., Štefl, S., Rivinius, T., Baade, D., & Haubois, X. 2012, ApJ, 744, L15
Charles, P. A., & Coe, M. J. 2006, Optical, ultraviolet and infrared observations of X-ray binaries, ed. W. H. G. Lewin & M. van der Klis, 215–265, Cambridge University Press
Chen, W., Livio, M., & Gehrels, N. 1993, ApJ, 408, L5
Chen, W., Shrader, C. R., & Livio, M. 1997, ApJ, 491, 312
D'Angelo, C. R., & Spruit, H. C. 2010, MNRAS, 406, 1208
—. 2011, MNRAS, 416, 893
Dubus, G., Hameury, J.-M., & Lasota, J.-P. 2001, A&A, 373, 251
Dubus, G., Lasota, J.-P., Hameury, J.-M., & Charles, P. 1999, MNRAS, 303, 139
Duschl, W. J., Strittmatter, P. A., & Biermann, P. L. 2000, A&A, 357, 1123
Eggleton, P. P. 1983, ApJ, 268, 368
Ertan, Ü., & Alpar, M. A. 2002, A&A, 393, 205
Filipov, L. G. 1984, Advances in Space Research, 3, 305
Guadalupe, J. J., Pérez, M., Ruiz, F. J., & Varona, J. L. 1993, Journal of Mathematical Analysis and Applications, 173, 370
Hameury, J.-M., & Lasota, J.-P. 2005, A&A, 443, 283
Ichikawa, S., & Osaki, Y. 1994, PASJ, 46, 621
Ivanov, P. B., Papaloizou, J. C. B., & Polnarev, A. G. 1999, MNRAS, 307, 79
Kato, S., Fukue, J., & Mineshige, S. 1998, Black-hole accretion disks, Vol. Kyot
King, A. R., Pringle, J. E., & Livio, M. 2007, MNRAS, 376, 1740
King, A. R., & Ritter, H. 1998, MNRAS, 293, L42
Kornet, K., & Rozyczka, M. 2000, Acta Astronomica., 50, 163
Kotko, I., & Lasota, J.-P. 2012, A&A, 545, A115
Lasota, J.-P. 2001, New Astronomy Review, 45, 449
Lin, D. N. C., & Bodenheimer, P. 1982, ApJ, 262, 768
Lin, D. N. C., & Pringle, J. E. 1987, MNRAS, 225, 607
Lipunov, V. M. 1992, Astrophysics of Neutron Stars (Springer-Verlag, Berlin)
Lipunova, G. V., & Shakura, N. I. 2000, A&A, 356, 363
Lubow, S. H. 1991, ApJ, 381, 259
Lüst, R. Z. 1952, Zeitschrift Naturforschung Teil A, 7, 87
Lynden-Bell, D. 1969, Nature, 223, 690
Lynden-Bell, D., & Pringle, J. E. 1974, MNRAS, 168, 603
Lyubarskij, Y. E., & Shakura, N. I. 1987, Soviet Astronomy Letters, 13, 386
MacRobert, T. M. 1932, Proc. Roy. Soc. Edinburgh, 51, 116
Menou, K., Hameury, J.-M., Lasota, J.-P., & Narayan, R. 2000, MNRAS, 314, 498
Metzger, B. D., Rafikov, R. R., & Bochkarev, K. V. 2012, MNRAS, 423, 505
Meyer, F. 1984, A&A, 131, 303
Meyer, F., & Meyer-Hofmeister, E. 1984, A&A, 140, L35
Miller, J. M., & Rykoff, E. 2007, The Astronomer's Telegram, 1066, 1
Mineshige, S. 1994, ApJ, 431, L99
Novikov, I. D., & Thorne, K. S. 1973, in Black Holes (Les Astres Occlus), ed. C. Dewitt & B. S. Dewitt, 343–450, Gordon and Breach Science Publishers, Inc.
Ogilvie, G. I. 1999, MNRAS, 306, L9
—. 2002, MNRAS, 331, 1053
Okazaki, A. T. 2007, in Astronomical Society of the Pacific Conference Series, Vol. 367, Massive Stars in Interactive Binaries, ed. N. St.-Louis & A. F. J. Moffat, 485, Astronomical Society of the Pacific Conference Series
Paczynski, B. 1977, ApJ, 216, 822
Papaloizou, J., & Pringle, J. E. 1977, MNRAS, 181, 441
Pichardo, B., Sparke, L. S., & Aguilar, L. A. 2005, MNRAS, 359, 521
Prandtl, L. 1925, Z. angew. Math. Mech., 5, 136
Pringle, J. E. 1974, PhD thesis, , Univ. Cambridge, (1974)
—. 1981, ARA&A, 19, 137
—. 1991, MNRAS, 248, 754
Rafikov, R. R. 2013, ApJ, 774, 144
Shakura, N. I. 1973, Soviet Astronomy, 16, 756
Shakura, N. I., & Sunyaev, R. A. 1973, A&A, 24, 337
Shen, R.-F., & Matzner, C. D. 2014, ApJ, 784, 87
Smak, J. 2000, New Astronomy Rev., 44, 171
Sneddon, I. N. 1951, Fourier Transforms, International Series in Pure and Applied Mathematics (McGraw-Hill)
Sturner, S. J., & Shrader, C. R. 2005, ApJ, 625, 923
Suleimanov, V. F., Lipunova, G. V., & Shakura, N. I. 2007, Astronomy Reports, 51, 549
—. 2008, A&A, 491, 267
Syunyaev, R. A., & Shakura, N. I. 1977, Soviet Astronomy Letters, 3, 138
Tanaka, T. 2011, MNRAS, 410, 1007
Tanaka, T., Menou, K., & Haiman, Z. 2012, MNRAS, 420, 705
Watson, G. 1944, A Treatise on the Theory of Bessel Functions, Cambridge University Press
Weizsäcker, C. F. V. 1948, Zeitschrift Naturforschung Teil A, 3, 524
Whitehurst, R., & King, A. 1991, MNRAS, 249, 25
Wood, K. S., Titarchuk, L., Ray, P. S., Wolff, M. T., Lovellette, M. N., & Bandyopadhyay, R. M. 2001, ApJ, 563, 246
Wu, Y. X., Yu, W., Li, T. P., Maccarone, T. J., & Li, X. D. 2010, ApJ, 718, 620
Zdziarski, A. A., Kawabata, R., & Mineshige, S. 2009, MNRAS, 399, 1633
Zurita, C., Durant, M., Torres, M. A. P., Shahbaz, T., Casares, J., & Steeghs, D. 2008, ApJ, 681, 1458